# Supplementary Information for: A Model-Based Approach for Pulse Selection from Electrodermal Activity

Sandya Subramanian, *Student Member, IEEE*, Patrick L. Purdon, *Member, IEEE*, Riccardo Barbieri, *Senior Member, IEEE*, and Emery N. Brown, *Fellow, IEEE*

## RESULTS ON SIMULATED EDA DATA

TABLE S-I
RESULTS OF 50 RUNS OF OUR FRAMEWORK ON SIMULATED EDA DATA

| Run # | Noise Level | Mu | Lambda | # Pulses (true) | Final Thresh | # Pulses (extracted) | # Pulses matched | Recall | Precision | Est. mu (99% CI) | Est. lambda (99% CI) |
|---|---|---|---|---|---|---|---|---|---|---|---|
| 1 | 1e-2 | 20 | 8 | 161 | 0.025 | 160 | 157 | 0.975 | 0.981 | 22.397 ± 7.279 | 8.821 ± 2.544 |
| 2 | 1e-2 | 20 | 8 | 159 | 0.023 | 151 | 148 | 0.931 | 0.980 | 23.810 ± 7.790 | 9.805 ± 2.911 |
| 3 | 1e-2 | 20 | 8 | 206 | 0.023 | 196 | 194 | 0.942 | 0.990 | 18.327 ± 4.762 | 9.218 ± 2.402 |
| 4 | 1e-2 | 20 | 8 | 231 | 0.022 | 228 | 224 | 0.970 | 0.983 | 15.548 ± 3.260* | 10.320 ± 2.494 |
| 5 | 1e-2 | 20 | 8 | 184 | 0.025 | 183 | 181 | 0.984 | 0.989 | 19.705 ± 5.427 | 9.451 ± 2.549 |
| 6 | 1e-2 | 20 | 10 | 180 | 0.023 | 176 | 173 | 0.961 | 0.983 | 20.450 ± 5.737 | 9.826 ± 2.702 |
| 7 | 1e-2 | 20 | 10 | 170 | 0.035 | 168 | 167 | 0.982 | 0.994 | 21.261 ± 6.062 | 10.363 ± 2.917 |
| 8 | 1e-2 | 20 | 10 | 216 | 0.05 | 208 | 206 | 0.954 | 0.990 | 17.197 ± 3.592 | 12.611 ± 3.190 |
| 9 | 1e-2 | 20 | 10 | 183 | 0.03 | 177 | 177 | 0.967 | 1.00 | 20.353 ± 5.158 | 11.916 ± 3.268 |
| 10 | 1e-2 | 20 | 10 | 163 | 0.022 | 163 | 161 | 0.988 | 0.988 | 22.011 ± 5.849 | 12.728 ± 3.637 |
| 11 | 1e-2 | 15 | 5 | 279 | 0.021 | 249 | 244 | 0.875 | 0.980 | 14.399 ± 3.350 | 7.111 ± 1.644* |
| 12 | 1e-2 | 15 | 5 | 260 | 0.022 | 232 | 228 | 0.877 | 0.983 | 15.543 ± 3.700 | 7.869 ± 1.885* |
| 13 | 1e-2 | 15 | 5 | 237 | 0.019 | 225 | 208 | 0.878 | 0.924 | 16.004 ± 3.933 | 7.840 ± 1.907* |
| 14 | 1e-2 | 15 | 5 | 255 | 0.022 | 237 | 232 | 0.910 | 0.979 | 15.170 ± 3.656 | 7.337 ± 1.739* |
| 15 | 1e-2 | 15 | 5 | 261 | 0.022 | 246 | 241 | 0.923 | 0.980 | 14.570 ± 3.515 | 6.774 ± 1.576* |
| 16 | 1e-2 | 20 | 5 | 164 | 0.021 | 152 | 145 | 0.884 | 0.954 | 23.385 ± 8.106 | 8.522 ± 2.522* |
| 17 | 1e-2 | 20 | 5 | 203 | 0.02 | 186 | 175 | 0.862 | 0.941 | 19.057 ± 5.450 | 8.340 ± 2.231* |
| 18 | 1e-2 | 20 | 5 | 172 | 0.025 | 154 | 151 | 0.878 | 0.981 | 23.177 ± 7.501 | 9.563 ± 2.812* |
| 19 | 1e-2 | 20 | 5 | 161 | 0.023 | 153 | 148 | 0.919 | 0.967 | 23.478 ± 8.188 | 8.398 ± 2.477* |
| 20 | 1e-2 | 20 | 5 | 216 | 0.023 | 198 | 195 | 0.903 | 0.985 | 18.127 ± 5.185 | 7.449 ± 1.932* |
| 21 | 1e-2 | 30 | 15 | 109 | 0.03 | 110 | 109 | 1.00 | 0.991 | 32.531 ± 11.329 | 16.230 ± 5.646 |
| 22 | 1e-2 | 30 | 15 | 154 | 0.065 | 152 | 151 | 0.981 | 0.993 | 23.054 ± 6.157* | 14.155 ± 4.189 |
| 23 | 1e-2 | 30 | 15 | 108 | 0.045 | 107 | 107 | 0.991 | 1.00 | 33.629 ± 13.602 | 12.788 ± 4.511 |
| 24 | 1e-2 | 30 | 15 | 131 | 0.025 | 131 | 128 | 0.977 | 0.977 | 27.274 ± 8.587 | 13.981 ± 4.457 |
| 25 | 1e-2 | 30 | 15 | 129 | 0.06 | 127 | 127 | 0.985 | 1.00 | 26.862 ± 7.138 | 19.940 ± 6.456 |
| 26 | 1e-2 | 25 | 10 | 150 | 0.024 | 149 | 148 | 0.987 | 0.993 | 23.788 ± 7.409 | 10.954 ± 3.274 |
| 27 | 1e-2 | 25 | 10 | 142 | 0.065 | 139 | 138 | 0.972 | 0.993 | 25.971 ± 8.548 | 11.480 ± 3.553 |
| 28 | 1e-2 | 25 | 10 | 123 | 0.03 | 119 | 118 | 0.959 | 0.992 | 30.229 ± 11.153 | 12.422 ± 4.155 |
| 29 | 1e-2 | 25 | 10 | 135 | 0.03 | 134 | 133 | 0.985 | 0.993 | 25.777 ± 8.473 | 11.851 ± 3.735 |
| 30 | 1e-2 | 25 | 10 | 141 | 0.03 | 139 | 137 | 0.972 | 0.986 | 25.980 ± 8.747 | 10.976 ± 3.397 |
| 31 | 5e-3 | 25 | 10 | 156 | 0.011 | 158 | 149 | 0.955 | 0.943 | 22.499 ± 7.246 | 9.138 ± 2.653 |
| 32 | 5e-3 | 25 | 10 | 158 | 0.08 | 142 | 142 | 0.899 | 1.00 | 25.481 ± 7.049 | 15.608 ± 4.779* |
| 33 | 5e-3 | 25 | 10 | 138 | 0.012 | 140 | 136 | 0.986 | 0.971 | 25.679 ± 9.649 | 8.648 ± 2.667 |
| 34 | 5e-3 | 25 | 10 | 135 | 0.075 | 123 | 122 | 0.904 | 0.992 | 28.442 ± 9.495 | 13.812 ± 4.544 |
| 35 | 5e-3 | 25 | 10 | 153 | 0.065 | 143 | 143 | 0.935 | 1.00 | 24.936 ± 6.969 | 14.859 ± 4.534* |
| 36 | 5e-3 | 15 | 10 | 266 | 0.018 | 260 | 260 | 0.977 | 1.00 | 13.866 ± 2.424 | 11.619 ± 2.629 |
| 37 | 5e-3 | 15 | 10 | 231 | 0.012 | 234 | 229 | 0.991 | 0.979 | 15.321 ± 3.055 | 10.958 ± 2.614 |
| 38 | 5e-3 | 15 | 10 | 211 | 0.018 | 208 | 206 | 0.976 | 0.990 | 17.345 ± 3.991 | 10.486 ± 2.653 |
| 39 | 5e-3 | 15 | 10 | 216 | 0.04 | 207 | 207 | 0.958 | 1.00 | 17.252 ± 3.379 | 14.458 ± 3.667* |
| 40 | 5e-3 | 15 | 10 | 213 | 0.014 | 212 | 206 | 0.967 | 0.972 | 16.860 ± 3.727 | 10.835 ± 2.715 |

| | | | | | | | | | | | |
|---|---|---|---|---|---|---|---|---|---|---|---|
| 41 | 3e-2 | 20 | 12 | 165 | 0.065 | 159 | 155 | 0.939 | 0.975 | 22.300 ± 5.481 | 15.454 ± 4.472 |
| 42 | 3e-2 | 20 | 12 | 190 | 0.06 | 191 | 186 | 0.979 | 0.974 | 18.530 ± 3.796 | 15.387 ± 4.062 |
| 43 | 3e-2 | 20 | 12 | 192 | 0.07 | 186 | 182 | 0.948 | 0.979 | 19.219 ± 4.239 | 14.135 ± 3.782 |
| 44 | 3e-2 | 20 | 12 | 164 | 0.135 | 156 | 155 | 0.945 | 0.994 | 23.034 ± 5.670 | 16.222 ± 4.739 |
| 45 | 3e-2 | 20 | 12 | 146 | 0.085 | 135 | 133 | 0.911 | 0.985 | 25.680 ± 7.102 | 16.555 ± 5.199 |
| 46 | 3e-2 | 25 | 15 | 140 | 0.06 | 155 | 138 | 0.986 | 0.890 | 22.759 ± 5.098 | 19.482 ± 5.710 |
| 47 | 3e-2 | 25 | 15 | 128 | 0.08 | 124 | 122 | 0.953 | 0.984 | 28.129 ± 8.017 | 18.590 ± 6.091 |
| 48 | 3e-2 | 25 | 15 | 144 | 0.075 | 146 | 144 | 1.00 | 0.986 | 24.598 ± 6.917 | 14.183 ± 4.283 |
| 49 | 3e-2 | 25 | 15 | 141 | 0.065 | 140 | 138 | 0.979 | 0.986 | 25.655 ± 6.598 | 18.443 ± 5.687 |
| 50 | 3e-2 | 25 | 15 | 119 | 0.075 | 117 | 117 | 0.983 | 1.00 | 30.570 ± 10.648 | 14.334 ± 4.835 |

# = number, Noise level = Standard deviation of noise, Mu = scale parameter of inverse Gaussian distribution, Lambda = shape parameter of inverse Gaussian distribution, # Pulses (true) = number of true pulses, Final thresh = final prominence threshold used, # Pulses extracted = number of pulses extracted by our framework, # Pulses matched = number of pulses matched in time between the true and extracted pulses, Recall = proportion of true pulses that were extracted by our framework, Precision = proportion of pulses extracted by our framework that were true pulses, Est. mu (99% CI) = estimated value of scale parameter of inverse Gaussian distribution reported as a 99% confidence interval, Est. lambda (99% CI) = estimated value of shape parameter of inverse Gaussian reported as a 99% confidence interval, * indicates that the true parameter value was not captured within the 99% confidence interval for that run

TABLE S-II
SUMMARY OF 50 RUNS OF OUR FRAMEWORK ON SIMULATED EDA DATA BY NOISE LEVEL

| Noise Level | Final Thresh (95% CI) | Recall (95% CI) | Precision (95% CI) |
|---|---|---|---|
| 1e-2 | 0.030 ± 0.005 | 0.946 ± 0.016 | 0.982 ± 0.006 |
| 5e-3 | 0.035 ± 0.018 | 0.955 ± 0.020 | 0.985 ± 0.012 |
| 3e-2 | 0.077 ± 0.014 | 0.962 ± 0.017 | 0.975 ± 0.019 |
| Overall | 0.040 ± 0.007 | 0.951 ± 0.011 | 0.981 ± 0.006 |

Noise level = Standard deviation of noise, Final thresh (95% CI) = final prominence threshold used reported as a 95% confidence interval, Sensitivity (95% CI) = proportion of true pulses that were extracted by our framework reported as a 95% confidence interval, Positive predictive value (95% CI) = proportion of pulses extracted by our framework that were true pulses reported as a 95% confidence interval

# AWAKE AND AT REST COHORT

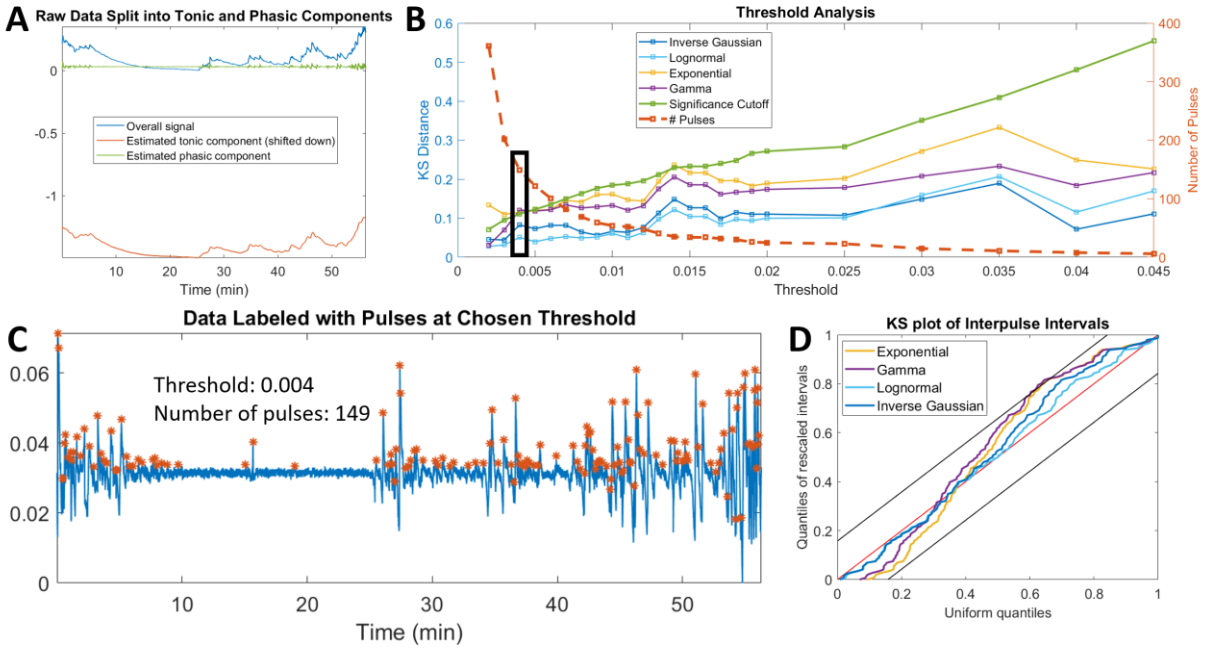


Fig. S1. Results for Subject S1 from the awake and at rest cohort, showing agreement with the trends of the cohort as a whole. (a) Preprocessing of data by splitting into tonic and phasic components, (b) Screening of thresholds with chosen threshold marked with bolded rectangle, (c) Pulses extracted at chosen threshold, (d) Full KS-plot showing goodness-of-fit at chosen threshold

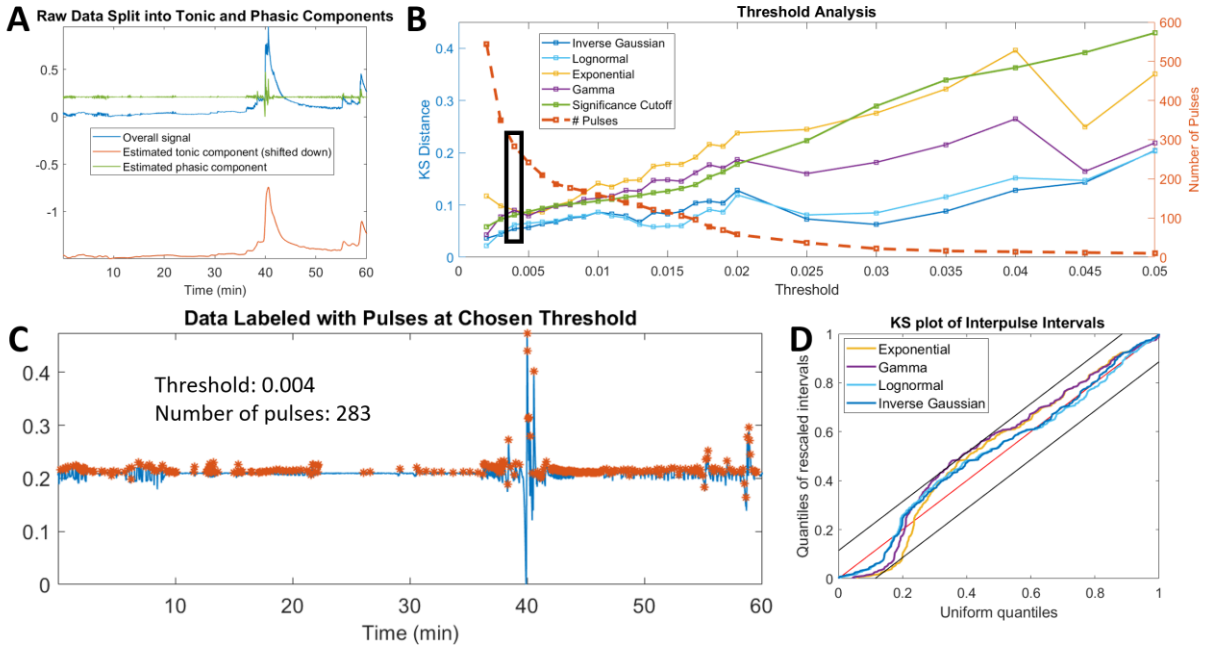


Fig. S2. Results for Subject S2 from the awake and at rest cohort, showing agreement with the trends of the cohort as a whole. (a) Preprocessing of data by splitting into tonic and phasic components, (b) Screening of thresholds with chosen threshold marked with bolded rectangle, (c) Pulses extracted at chosen threshold, (d) Full KS-plot showing goodness-of-fit at chosen threshold

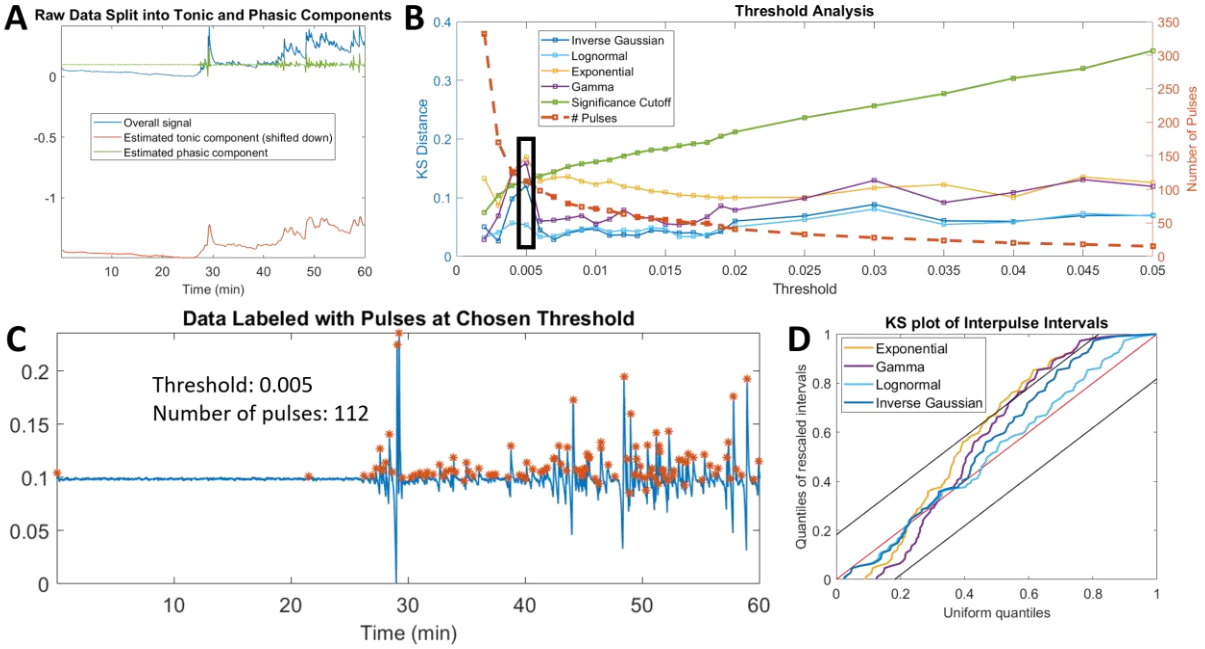


Fig. S3. Results for Subject S3 from the awake and at rest cohort, showing agreement with the trends of the cohort as a whole. (a) Preprocessing of data by splitting into tonic and phasic components, (b) Screening of thresholds with chosen threshold marked with bolded rectangle, (c) Pulses extracted at chosen threshold, (d) Full KS-plot showing goodness-of-fit at chosen threshold

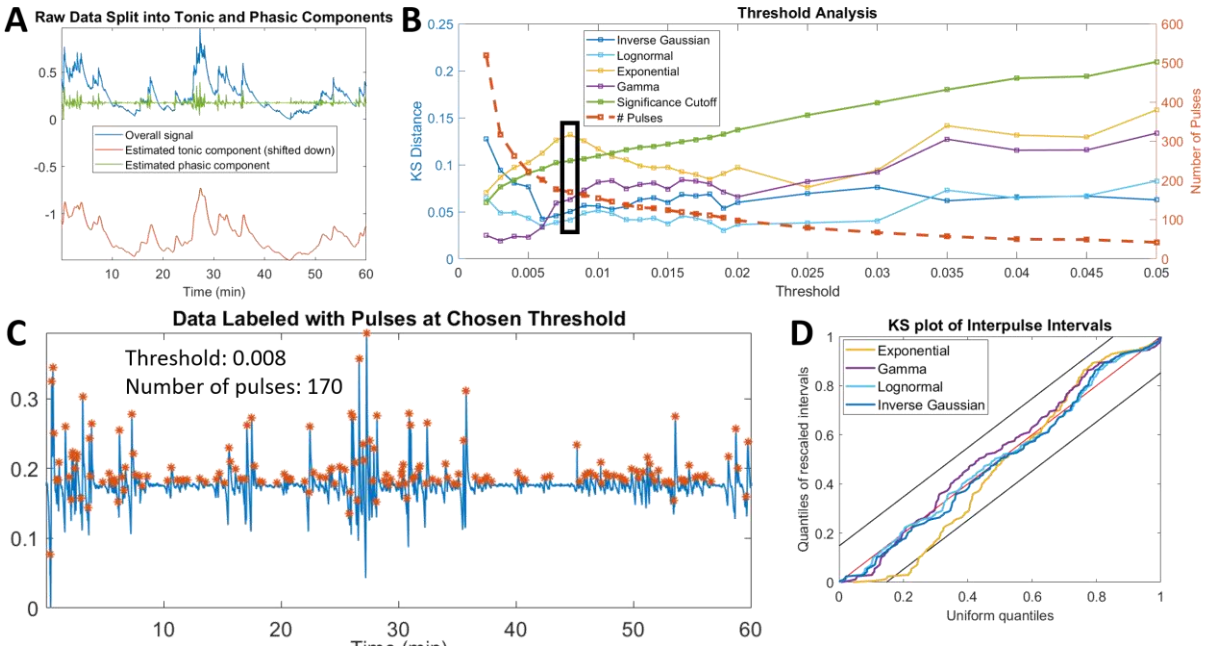


Fig. S4. Results for Subject S4 from the awake and at rest cohort, showing agreement with the trends of the cohort as a whole. (a) Preprocessing of data by splitting into tonic and phasic components, (b) Screening of thresholds with chosen threshold marked with bolded rectangle, (c) Pulses extracted at chosen threshold, (d) Full KS-plot showing goodness-of-fit at chosen threshold

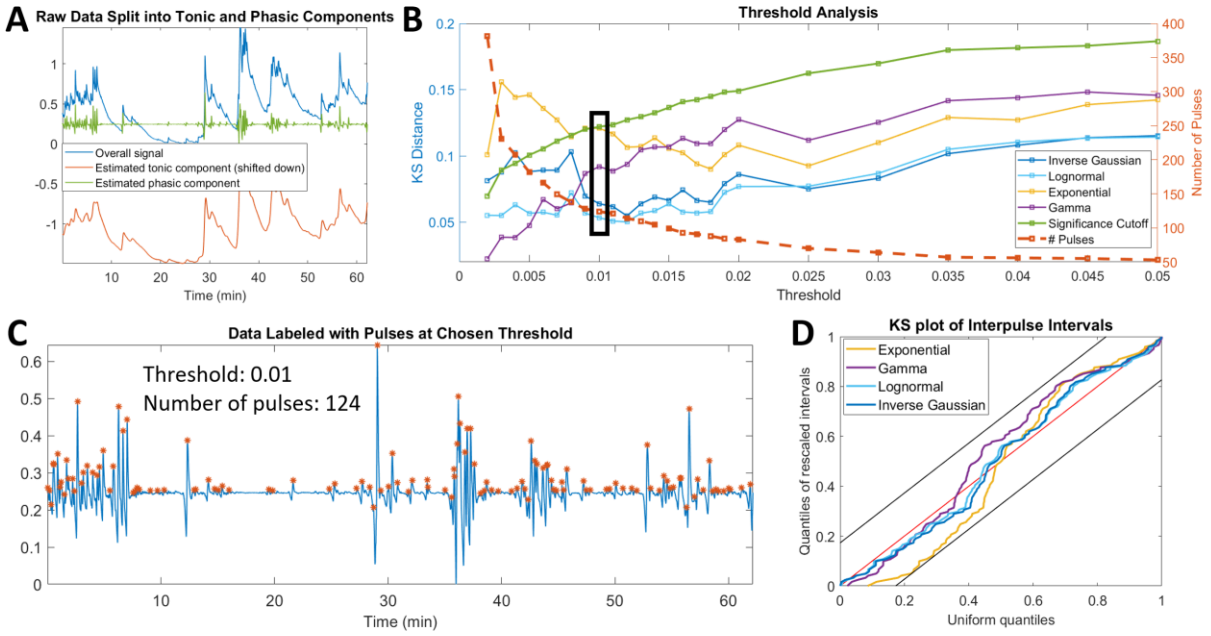


Fig. S5. Results for Subject S7 from the awake and at rest cohort, showing agreement with the trends of the cohort as a whole. (a) Preprocessing of data by splitting into tonic and phasic components, (b) Screening of thresholds with chosen threshold marked with bolded rectangle, (c) Pulses extracted at chosen threshold, (d) Full KS-plot showing goodness-of-fit at chosen threshold

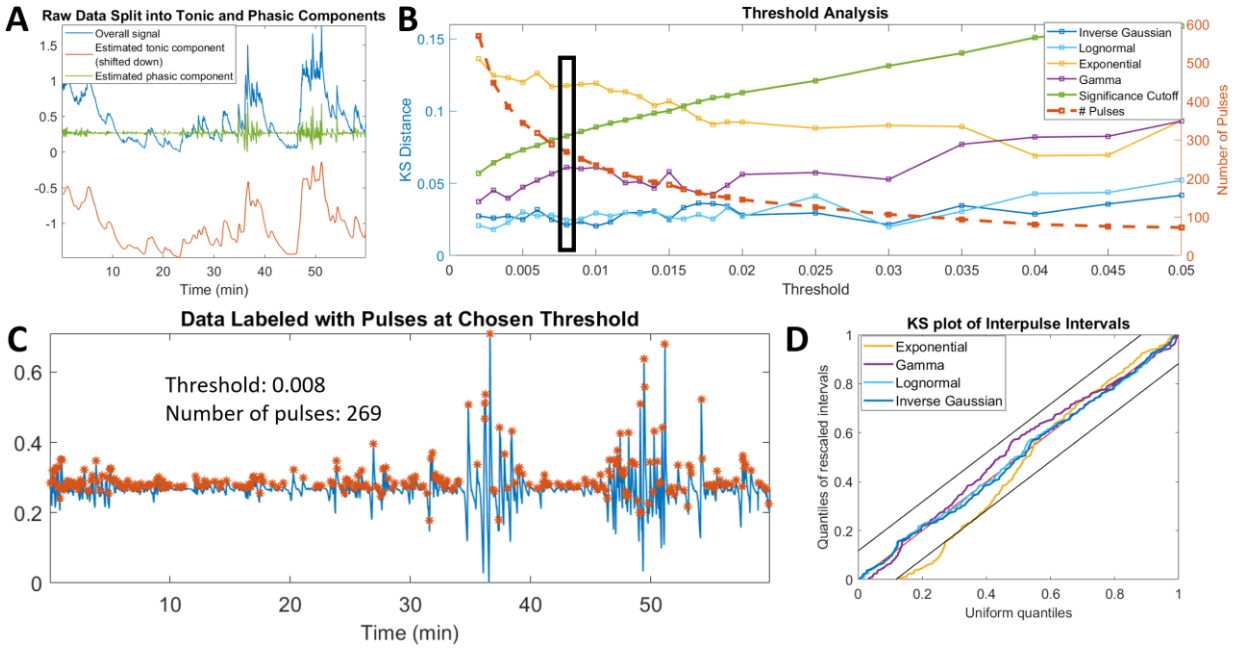


Fig. S6. Results for Subject S8 from the awake and at rest cohort, showing agreement with the trends of the cohort as a whole. (a) Preprocessing of data by splitting into tonic and phasic components, (b) Screening of thresholds with chosen threshold marked with bolded rectangle, (c) Pulses extracted at chosen threshold, (d) Full KS-plot showing goodness-of-fit at chosen threshold

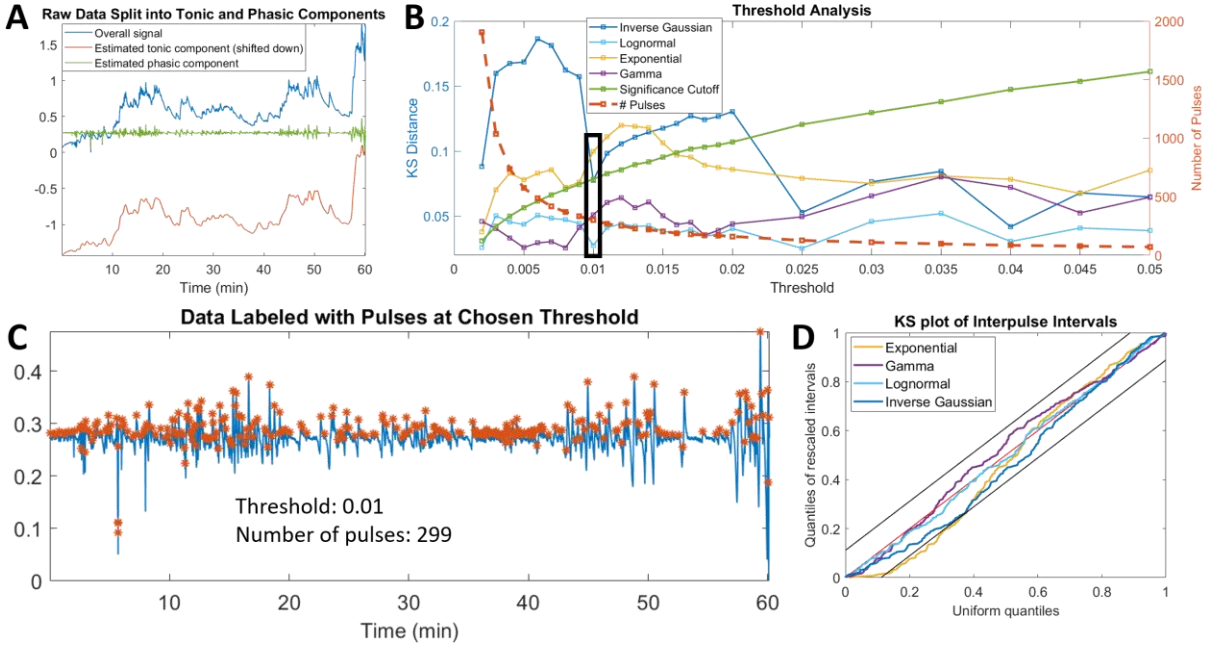


Fig. S7. Results for Subject S9 from the awake and at rest cohort, showing agreement with the trends of the cohort as a whole. (a) Preprocessing of data by splitting into tonic and phasic components, (b) Screening of thresholds with chosen threshold marked with bolded rectangle, (c) Pulses extracted at chosen threshold, (d) Full KS-plot showing goodness-of-fit at chosen threshold

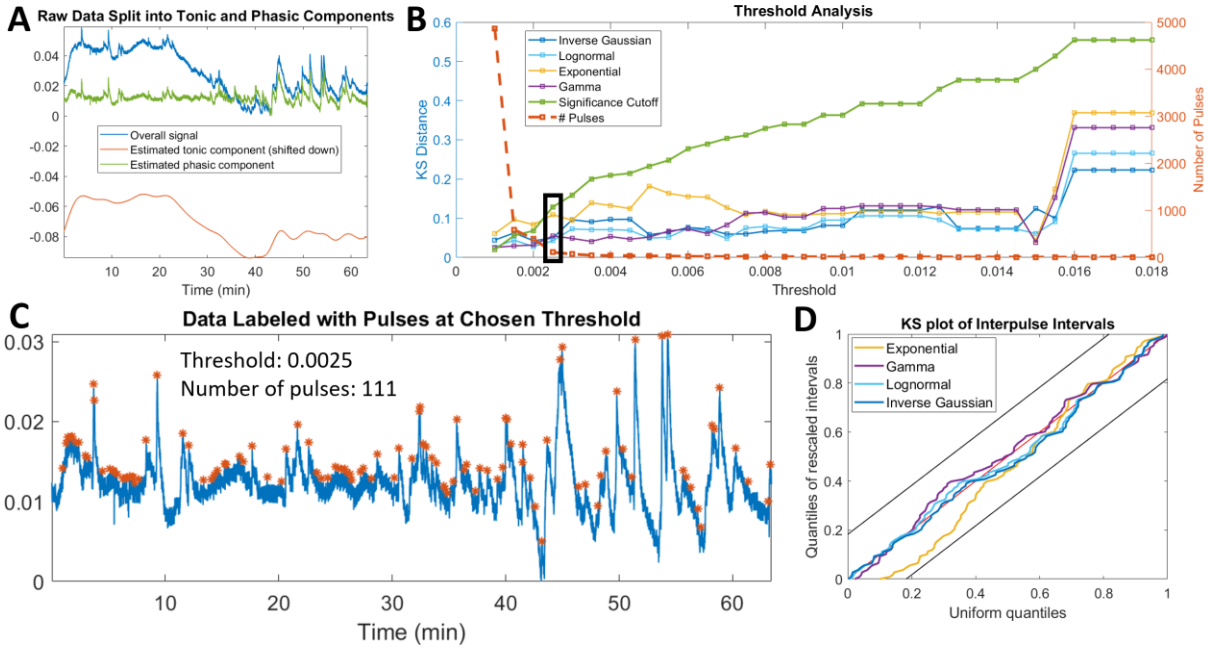


Fig. S8. Results for Subject S10 from the awake and at rest cohort, showing agreement with the trends of the cohort as a whole. (a) Preprocessing of data by splitting into tonic and phasic components, (b) Screening of thresholds with chosen threshold marked with bolded rectangle, (c) Pulses extracted at chosen threshold, (d) Full KS-plot showing goodness-of-fit at chosen threshold

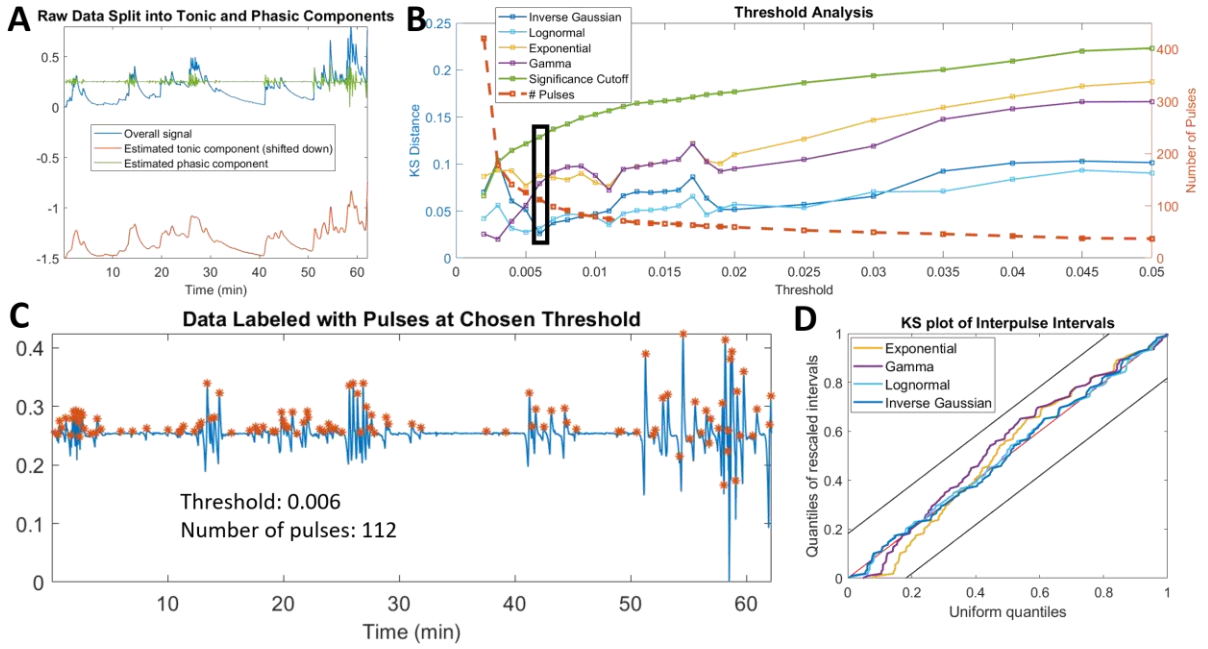


Fig. S9. Results for Subject S11 from the awake and at rest cohort, showing agreement with the trends of the cohort as a whole. (a) Preprocessing of data by splitting into tonic and phasic components, (b) Screening of thresholds with chosen threshold marked with bolded rectangle, (c) Pulses extracted at chosen threshold, (d) Full KS-plot showing goodness-of-fit at chosen threshold

# PROPOFOL SEDATION COHORT

TABLE S-III
AIC RESULTS FOR THE PROPOFOL SEDATION COHORT

| | Thresh | Num. pulses | IG | LogN | Gamma | Exp |
|---|---|---|---|---|---|---|
| **P1** | 0.035 | 727 | 4892.359 | **4862.670** | 5077.407 | 5159.771 |
| **P2** | 0.020 | 383 | **3232.026** | 3243.971 | 3370.773 | 3370.680 |
| **P3** | 0.035 | 762 | 5259.942 | **5259.534** | 5470.766 | 5468.826 |
| **P4** | 0.025 | 1010 | 7169.775 | **7130.224** | 7440.207 | 7440.261 |
| **P5** | 0.055 | 566 | 4293.377 | **4260.999** | 4400.896 | 4428.529 |
| **P6** | 0.020 | 838 | 5512.970 | **5490.560** | 5701.877 | 5772.100 |
| **P7** | 0.035 | 1250 | **7489.674** | 7498.297 | 7771.781 | 7866.955 |
| **P8** | 0.040 | 494 | **3837.628** | 3847.869 | 3991.711 | 3990.792 |
| **P9** | 0.055 | 575 | 4479.243 | **4448.334** | 4522.479 | 4570.867 |
| **P10** | 0.021 | 627 | **4617.829** | 4651.130 | 4874.572 | 4917.459 |
| **P11** | 0.030 | 778 | 5355.024 | **5332.838** | 5392.146 | 5523.467 |

The best model for each subject is indicated in bold.
Thresh = threshold, IG = inverse Gaussian, LogN = lognormal, Exp = exponential

TABLE S-IV
SETTLING RATE RESULTS FOR THE PROPOFOL SEDATION COHORT

| | IG | LogN | Gamma | Exp |
|---|---|---|---|---|
| **P1** | 0.047 | 0 | 0.125 | 0.078 |
| **P2** | 0.008 | 0 | 0.030 | 0.033 |
| **P3** | 0.021 | 0 | 0.076 | 0.075 |
| **P4** | 0.020 | 0 | 0.072 | 0.068 |
| **P5** | 0.023 | 0 | 0.073 | 0.054 |
| **P6** | 0.045 | 0 | 0.129 | 0.087 |
| **P7** | 0.058 | 0 | 0.170 | 0.117 |
| **P8** | 0.012 | 0 | 0.045 | 0.048 |
| **P9** | 0.023 | 0 | 0.076 | 0.051 |
| **P10** | 0.009 | 0 | 0.039 | 0.054 |
| **P11** | 0.045 | 0 | 0.140 | 0.078 |

IG = inverse Gaussian, LogN = lognormal, Exp = exponential

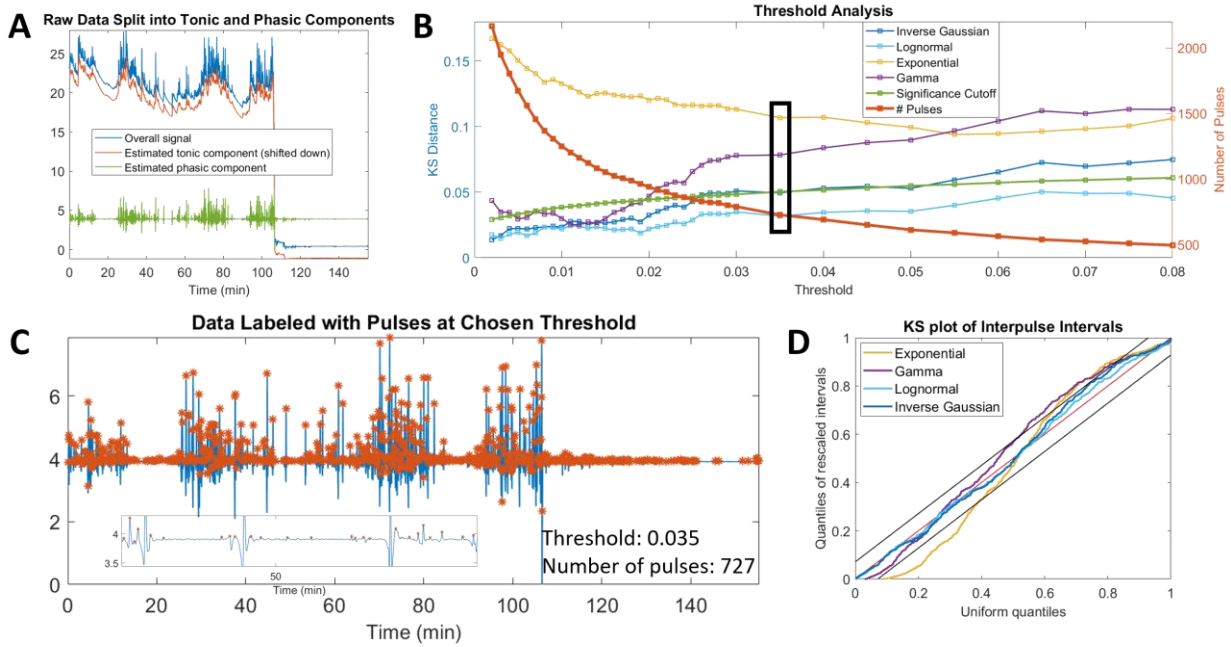


Fig. S10. Results for Subject P1 from the propofol sedation cohort, showing agreement with the trends of the cohort as a whole. (a) Preprocessing of data by splitting into tonic and phasic components, (b) Screening of thresholds with chosen threshold marked with bolded rectangle, (c) Pulses extracted at chosen threshold, (d) Full KS-plot showing goodness-of-fit at chosen threshold

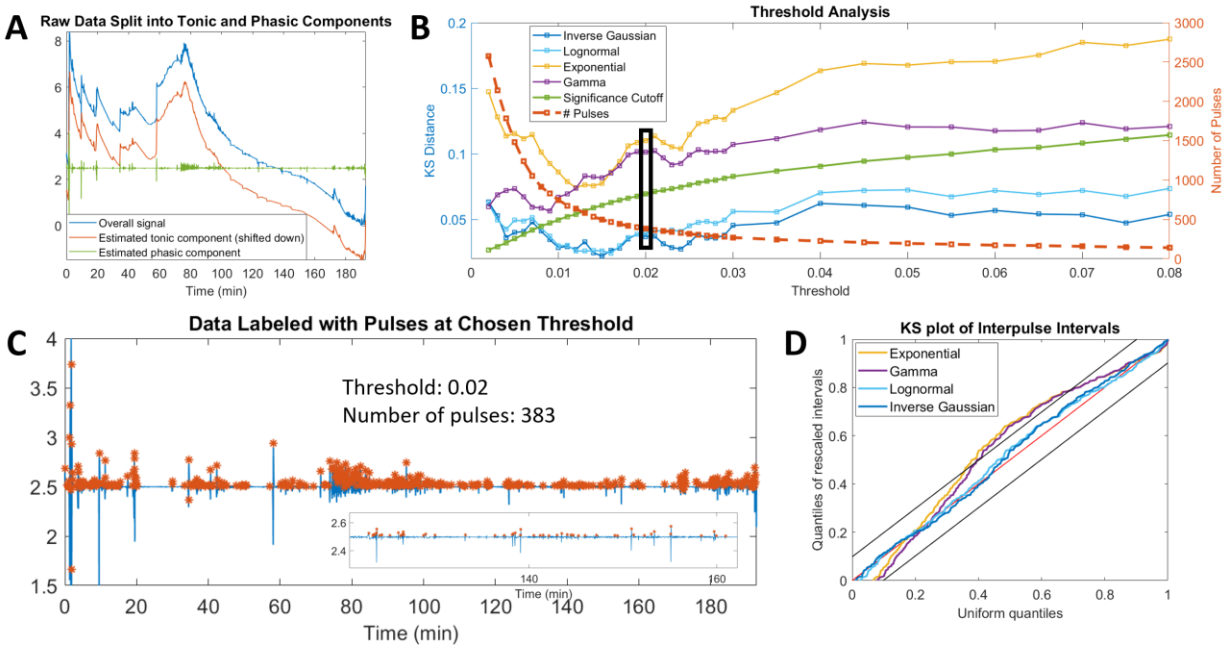


Fig. S11. Results for Subject P2 from the propofol sedation cohort, showing agreement with the trends of the cohort as a whole. (a) Preprocessing of data by splitting into tonic and phasic components, (b) Screening of thresholds with chosen threshold marked with bolded rectangle, (c) Pulses extracted at chosen threshold, (d) Full KS-plot showing goodness-of-fit at chosen threshold

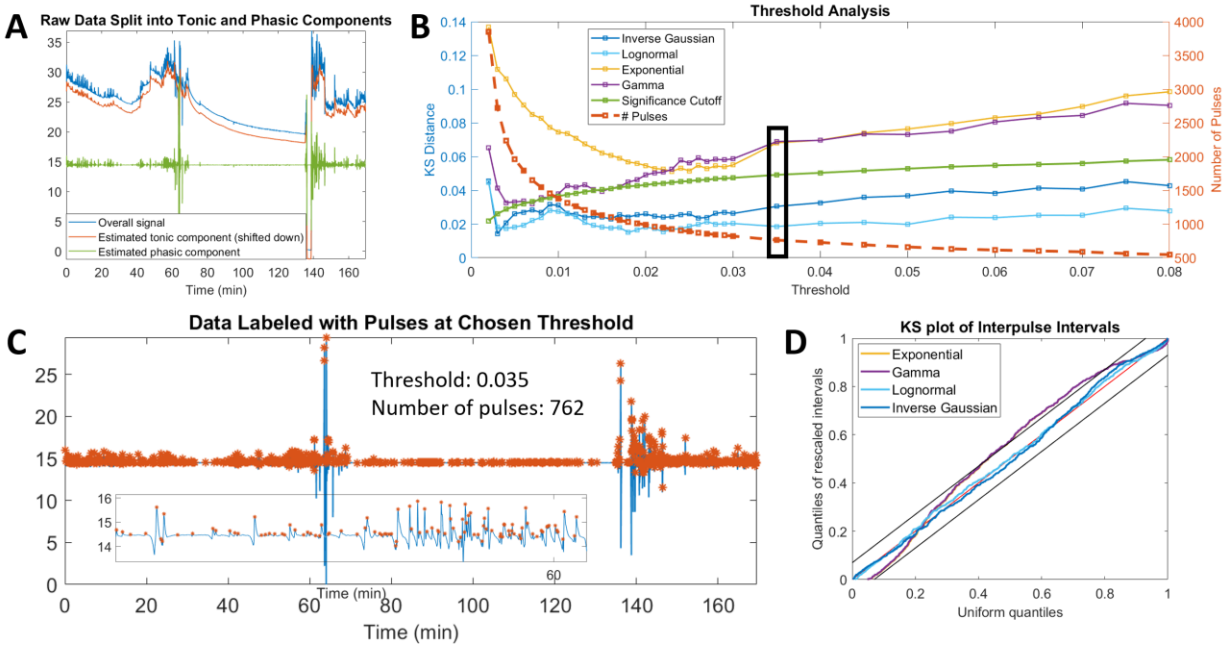


Fig. S12. Results for Subject P3 from the propofol sedation cohort, showing agreement with the trends of the cohort as a whole. (a) Preprocessing of data by splitting into tonic and phasic components, (b) Screening of thresholds with chosen threshold marked with bolded rectangle, (c) Pulses extracted at chosen threshold, (d) Full KS-plot showing goodness-of-fit at chosen threshold

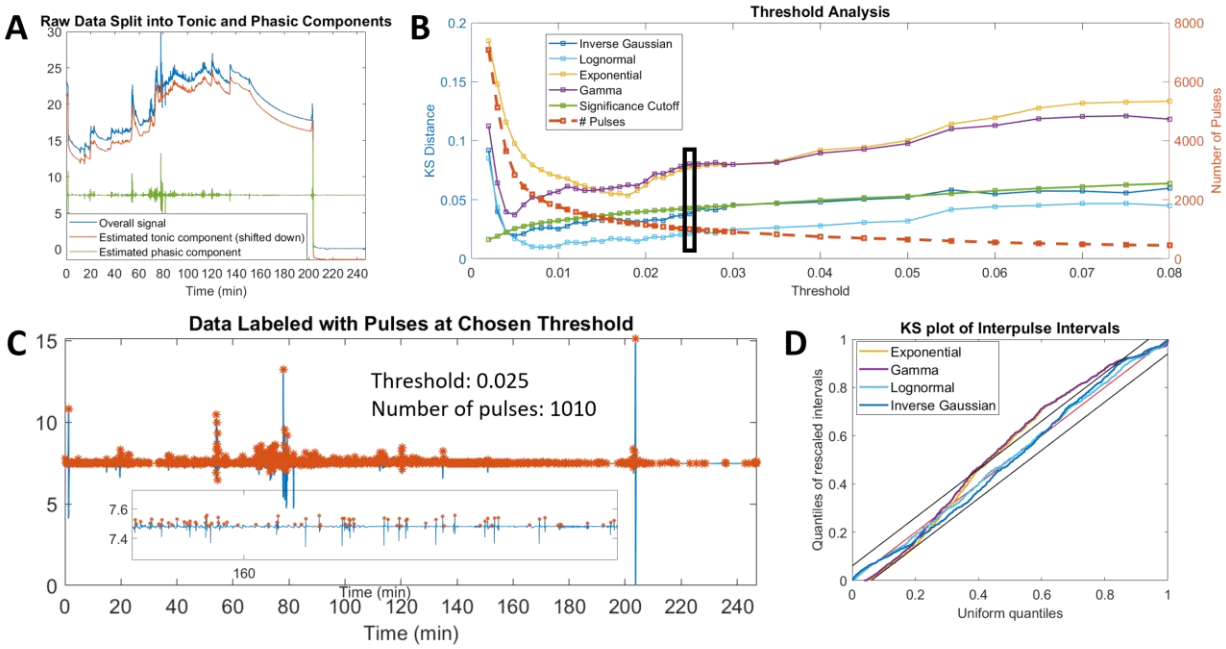


Fig. S13. Results for Subject P4 from the propofol sedation cohort, showing agreement with the trends of the cohort as a whole. (a) Preprocessing of data by splitting into tonic and phasic components, (b) Screening of thresholds with chosen threshold marked with bolded rectangle, (c) Pulses extracted at chosen threshold, (d) Full KS-plot showing goodness-of-fit at chosen threshold

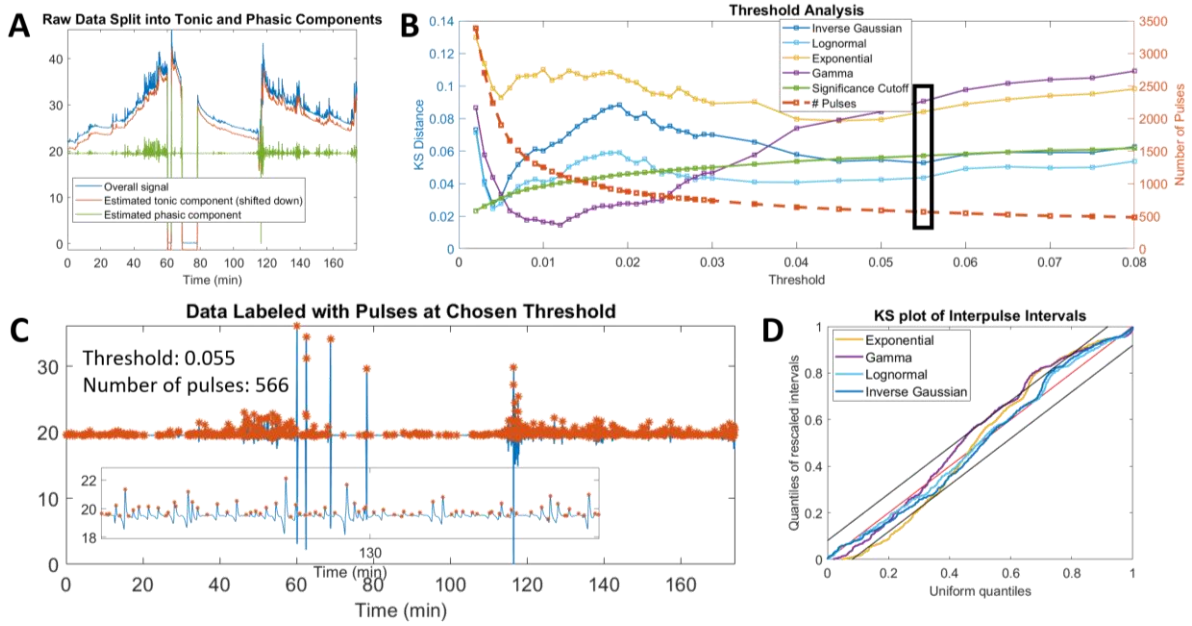


Fig. S14. Results for Subject P5 from the propofol sedation cohort, showing agreement with the trends of the cohort as a whole. (a) Preprocessing of data by splitting into tonic and phasic components, (b) Screening of thresholds with chosen threshold marked with bolded rectangle, (c) Pulses extracted at chosen threshold, (d) Full KS-plot showing goodness-of-fit at chosen threshold

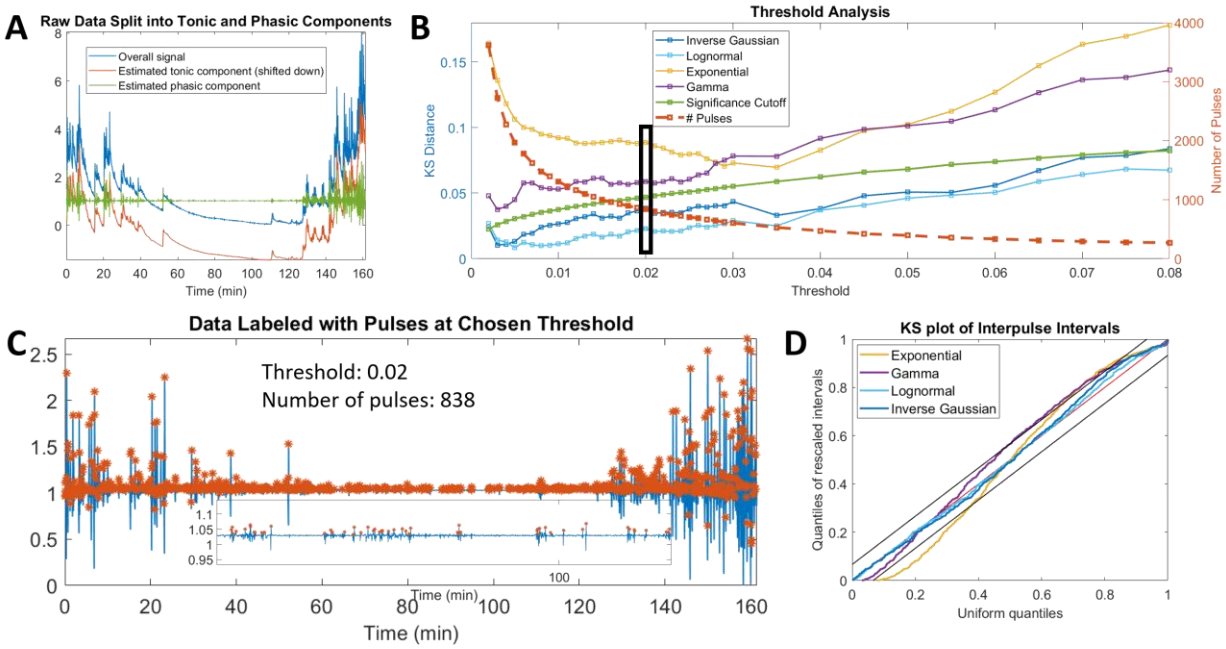


Fig. S15. Results for Subject P6 from the propofol sedation cohort, showing agreement with the trends of the cohort as a whole. (a) Preprocessing of data by splitting into tonic and phasic components, (b) Screening of thresholds with chosen threshold marked with bolded rectangle, (c) Pulses extracted at chosen threshold, (d) Full KS-plot showing goodness-of-fit at chosen threshold

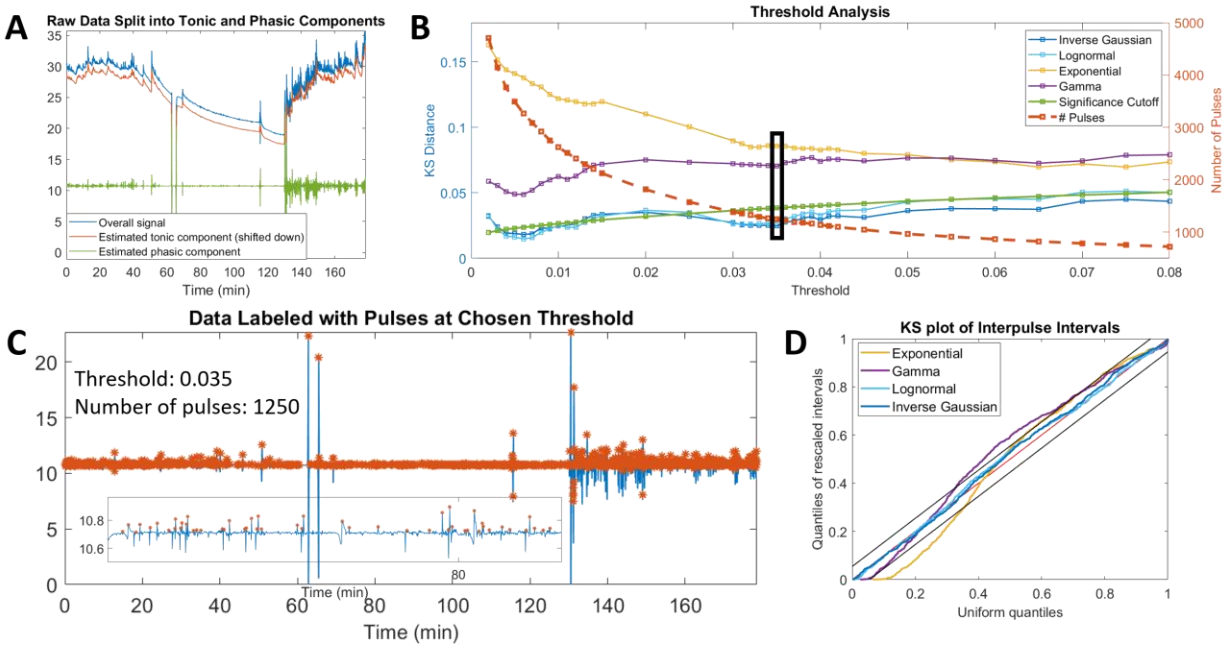


Fig. S16. Results for Subject P7 from the propofol sedation cohort, showing agreement with the trends of the cohort as a whole. (a) Preprocessing of data by splitting into tonic and phasic components, (b) Screening of thresholds with chosen threshold marked with bolded rectangle, (c) Pulses extracted at chosen threshold, (d) Full KS-plot showing goodness-of-fit at chosen threshold

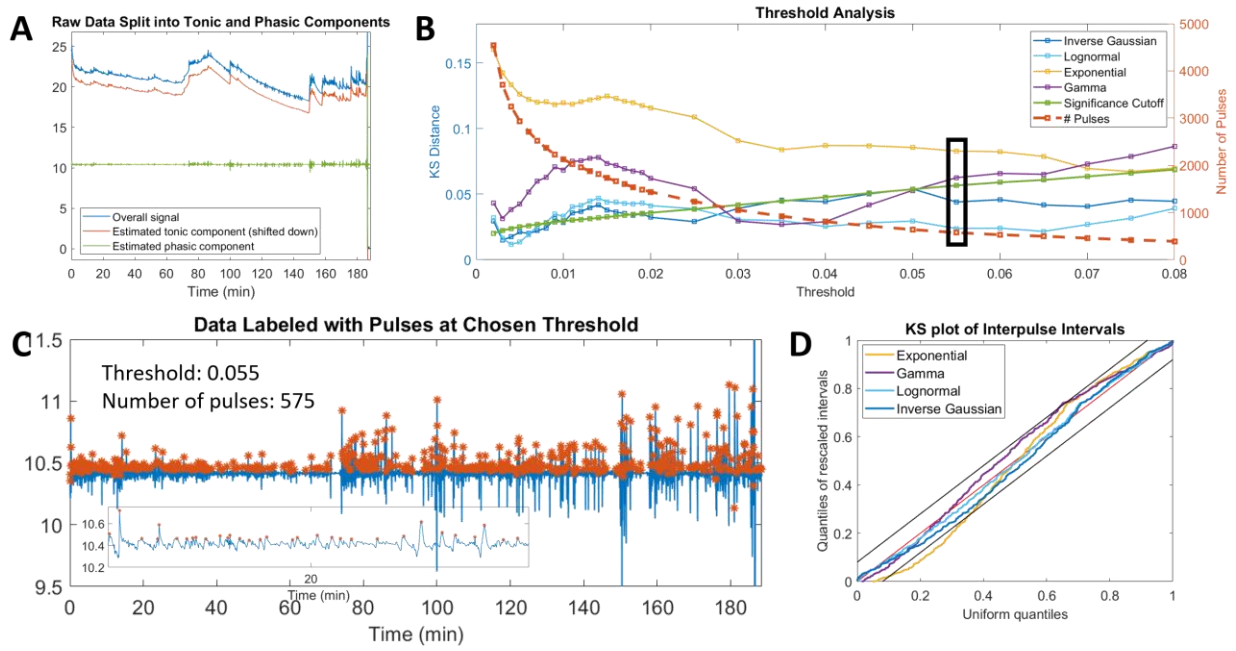


Fig. S17. Results for Subject P9 from the propofol sedation cohort, showing agreement with the trends of the cohort as a whole. (a) Preprocessing of data by splitting into tonic and phasic components, (b) Screening of thresholds with chosen threshold marked with bolded rectangle, (c) Pulses extracted at chosen threshold, (d) Full KS-plot showing goodness-of-fit at chosen threshold

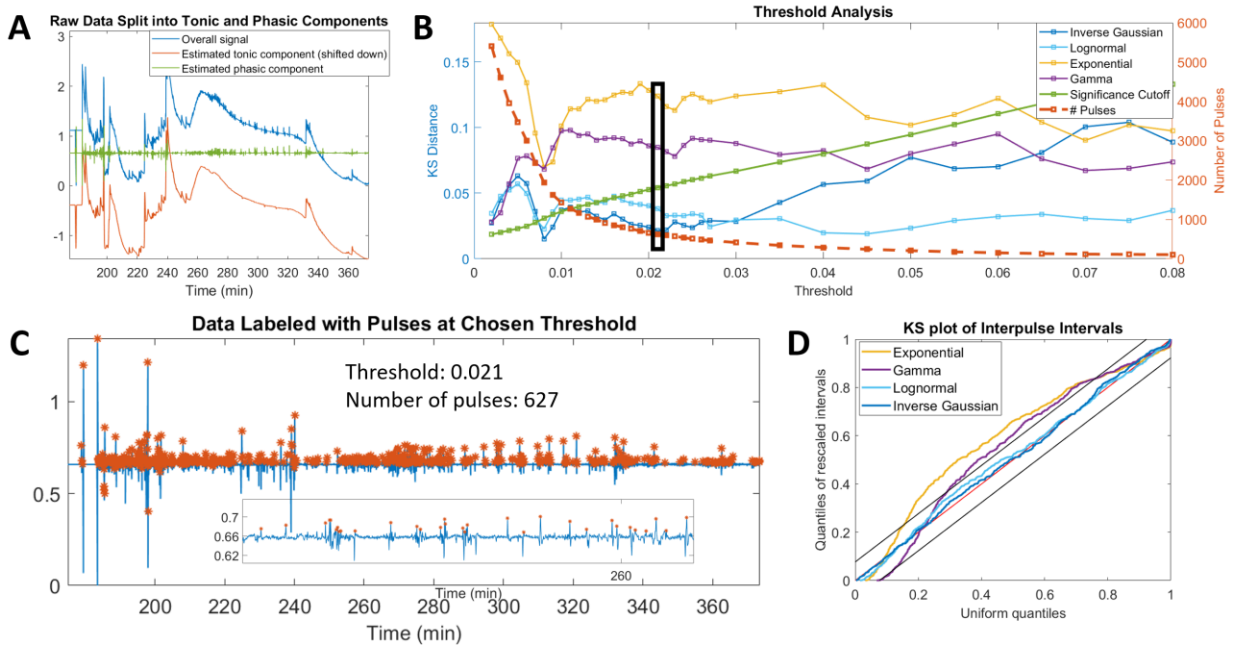


Fig. S18. Results for Subject P10 from the propofol sedation cohort, showing agreement with the trends of the cohort as a whole. (a) Preprocessing of data by splitting into tonic and phasic components, (b) Screening of thresholds with chosen threshold marked with bolded rectangle, (c) Pulses extracted at chosen threshold, (d) Full KS-plot showing goodness-of-fit at chosen threshold

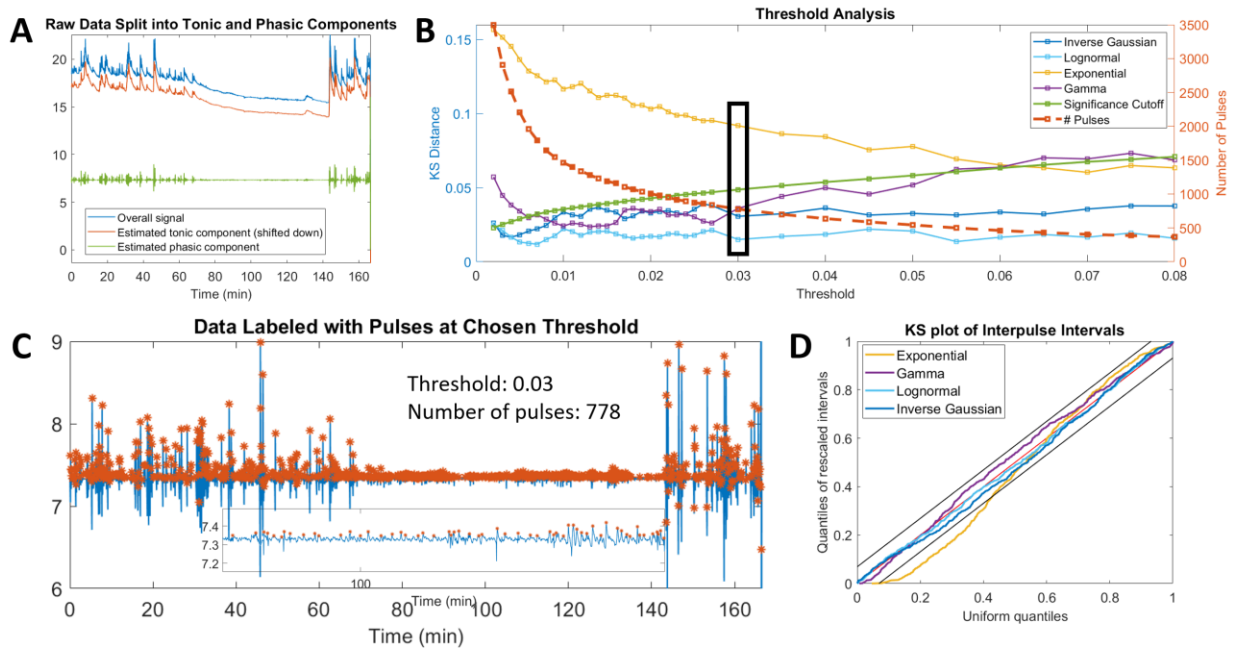


Fig. S19. Results for Subject P11 from the propofol sedation cohort, showing agreement with the trends of the cohort as a whole. (a) Preprocessing of data by splitting into tonic and phasic components, (b) Screening of thresholds with chosen threshold marked with bolded rectangle, (c) Pulses extracted at chosen threshold, (d) Full KS-plot showing goodness-of-fit at chosen threshold

# LEDALAB ALGORITHM RESULTS ON AWAKE AND AT REST COHORT

TABLE S-V
SUMMARY OF KS-DISTANCE RESULTS FOR THE AWAKE AND AT REST COHORT USING THE LEDALAB ALGORITHM

| | Num. pulses | Models under Sig. Cutoff |
|---|---|---|
| **S1** | 727 | IG |
| **S2** | 383 | -- |
| **S3** | 762 | -- |
| **S4** | 1010 | -- |
| **S5** | 566 | -- |
| **S6** | 838 | IG, LogN |
| **S7** | 1250 | -- |
| **S8** | 494 | -- |
| **S9** | 575 | LogN |
| **S10** | 627 | -- |
| **S11** | 778 | -- |

Sig. cutoff = significance cutoff, IG = inverse Gaussian, LogN = lognormal

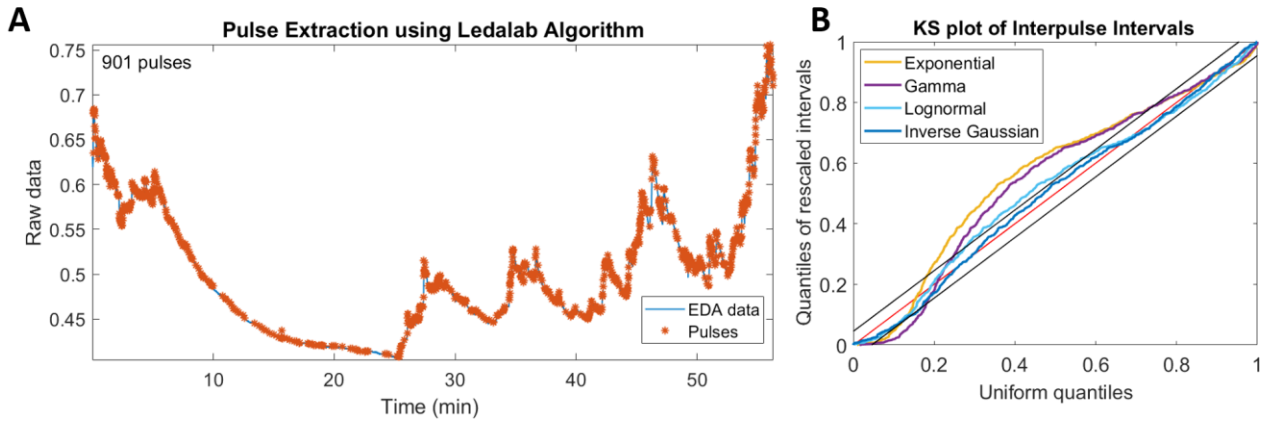


Fig. S20. (a) Pulse selection and (b) goodness-of-fit results using the Ledalab algorithm for Subject S1 from the awake and at rest cohort.

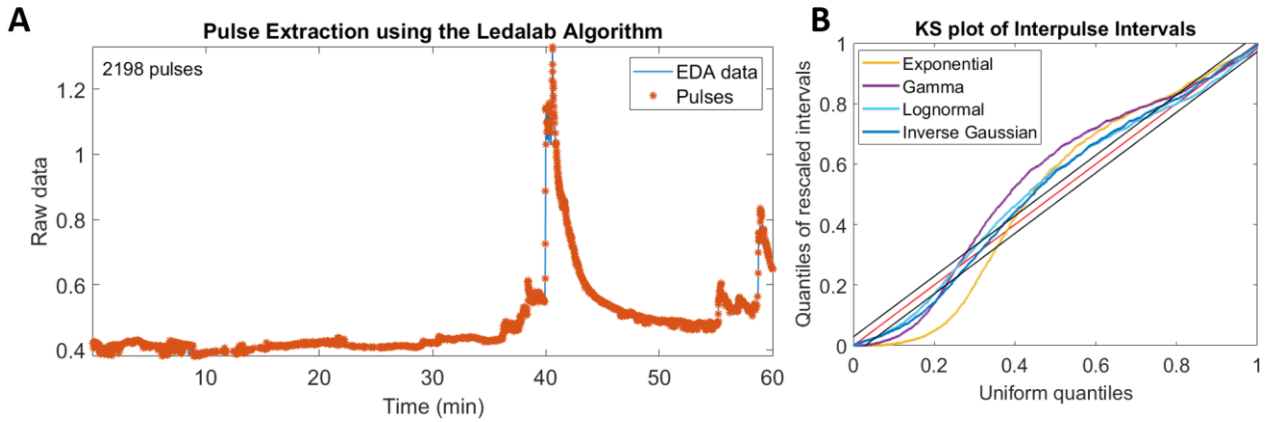


Fig. S21. (a) Pulse selection and (b) goodness-of-fit results using the Ledalab algorithm for Subject S2 from the awake and at rest cohort.

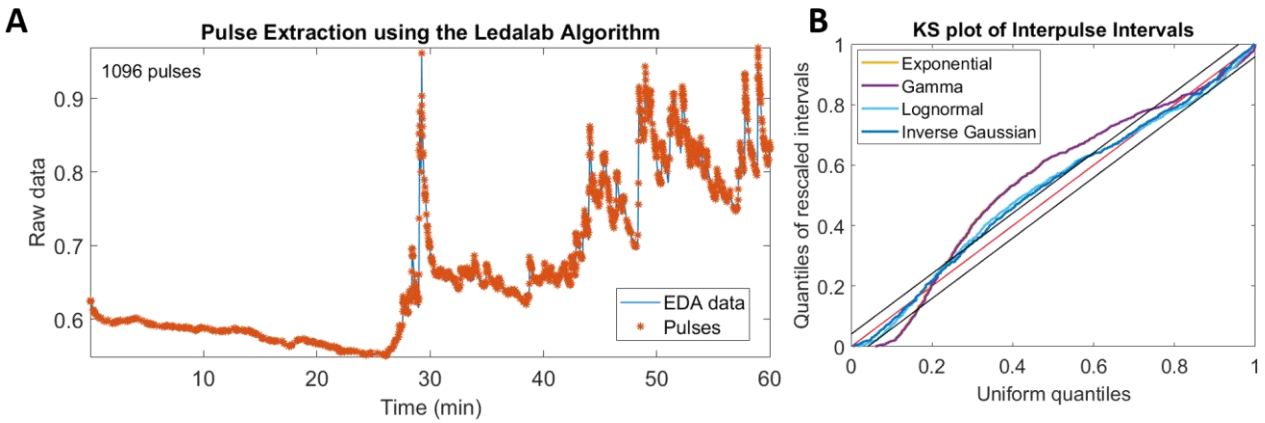


Fig. S22. (a) Pulse selection and (b) goodness-of-fit results using the Ledalab algorithm for Subject S3 from the awake and at rest cohort.

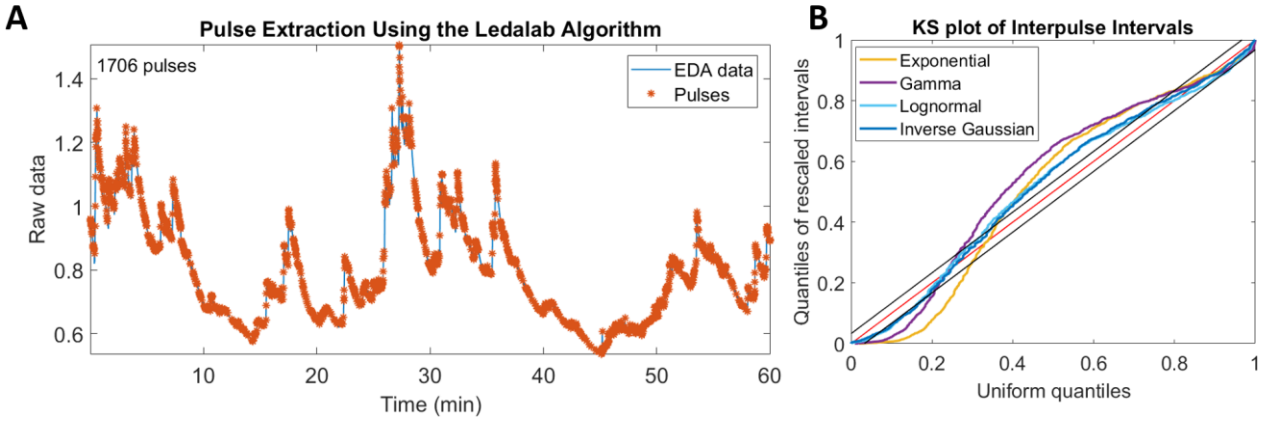


Fig. S23. (a) Pulse selection and (b) goodness-of-fit results using the Ledalab algorithm for Subject S4 from the awake and at rest cohort.

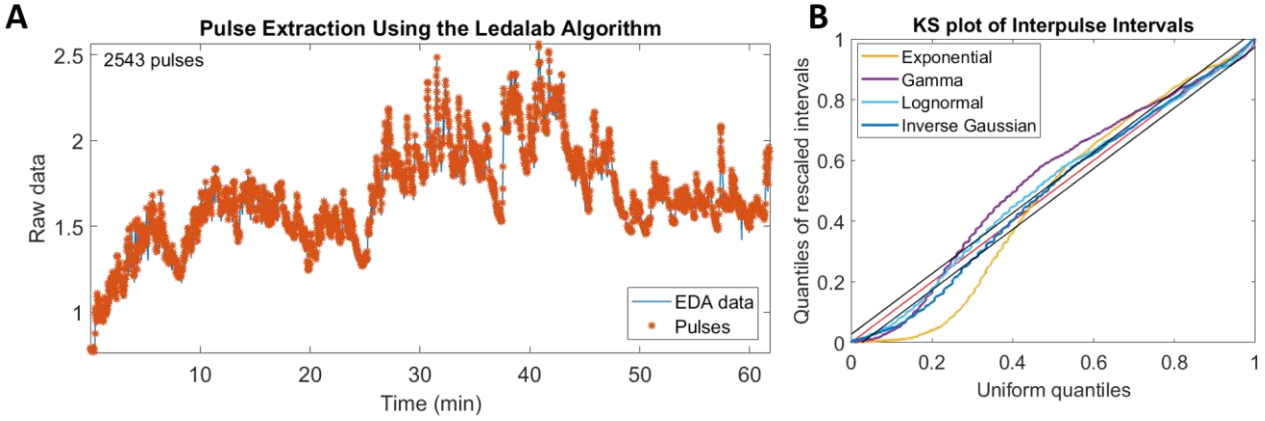


Fig. S24. (a) Pulse selection and (b) goodness-of-fit results using the Ledalab algorithm for Subject S5 from the awake and at rest cohort.

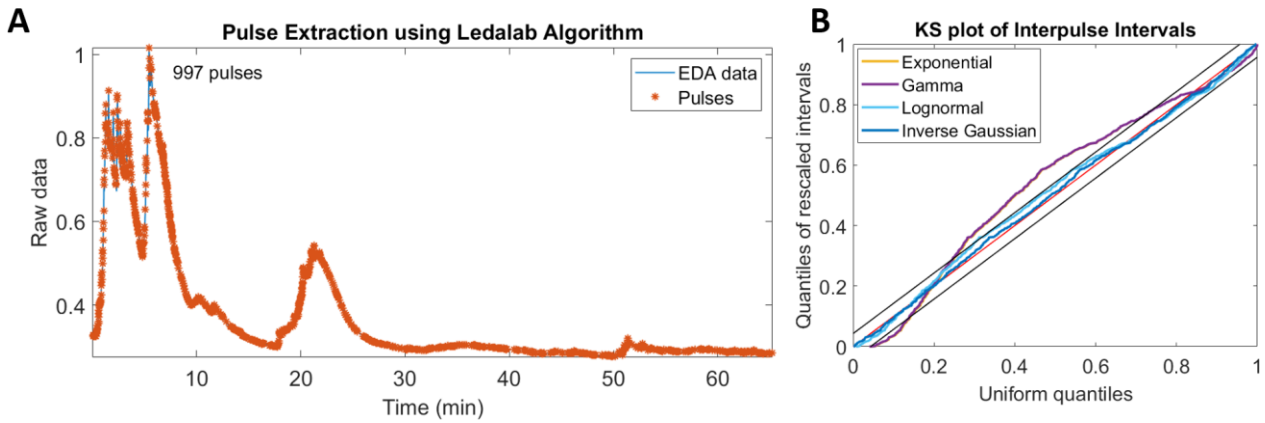


Fig. S25. (a) Pulse selection and (b) goodness-of-fit results using the Ledalab algorithm for Subject S6 from the awake and at rest cohort.

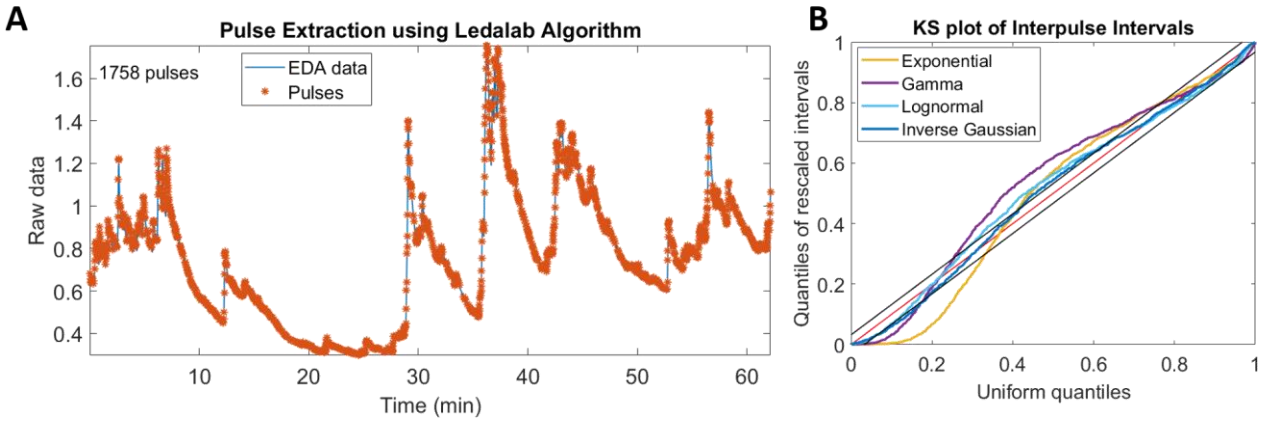


Fig. S26. (a) Pulse selection and (b) goodness-of-fit results using the Ledalab algorithm for Subject S7 from the awake and at rest cohort.

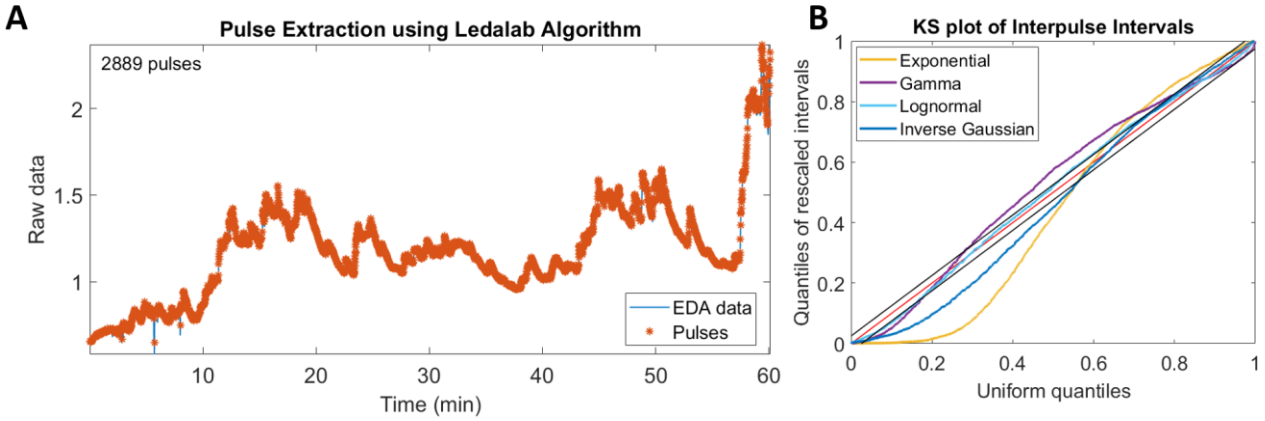


Fig. S27. (a) Pulse selection and (b) goodness-of-fit results using the Ledalab algorithm for Subject S9 from the awake and at rest cohort.

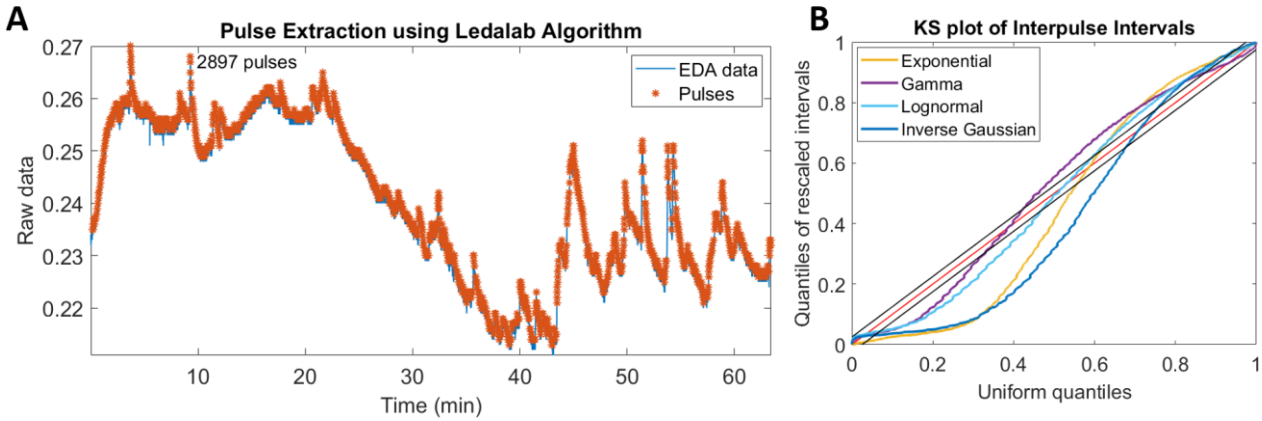


Fig. S29. (a) Pulse selection and (b) goodness-of-fit results using the Ledalab algorithm for Subject S10 from the awake and at rest cohort.

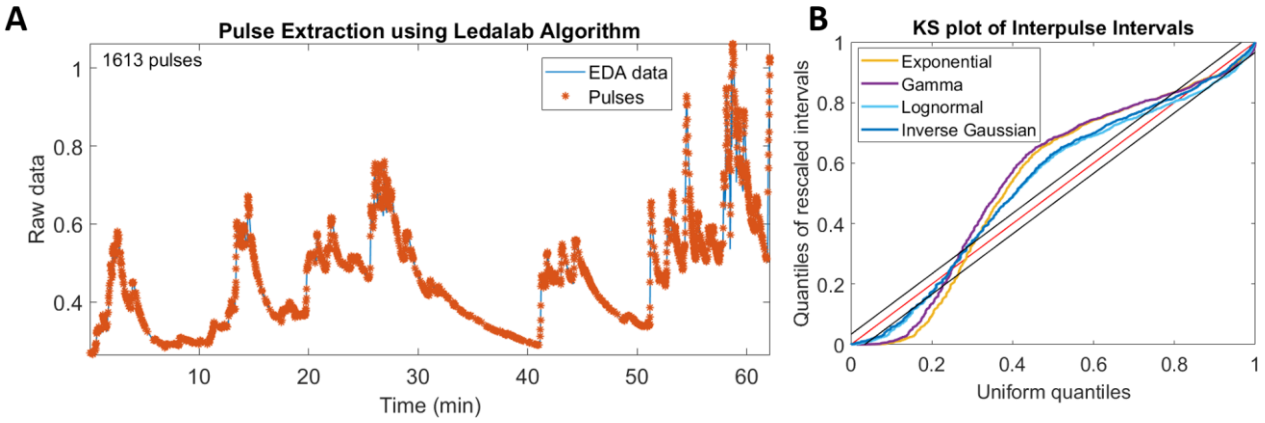


Fig. S28. (a) Pulse selection and (b) goodness-of-fit results using the Ledalab algorithm for Subject S11 from the awake and at rest cohort.

# cvxEDA ALGORITHM RESULTS ON AWAKE AND AT REST COHORT

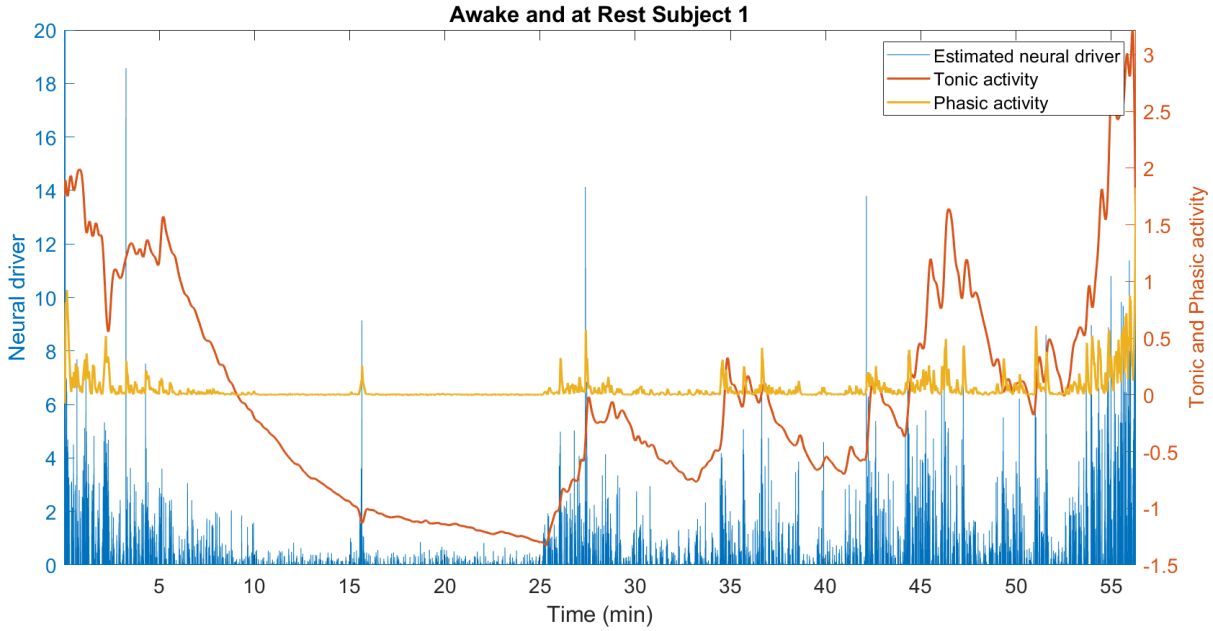


Fig. S30. Results using the cvxEDA algorithm for Subject S1 from the awake and at rest cohort, showing the tonic and phasic components and the estimated neural activity

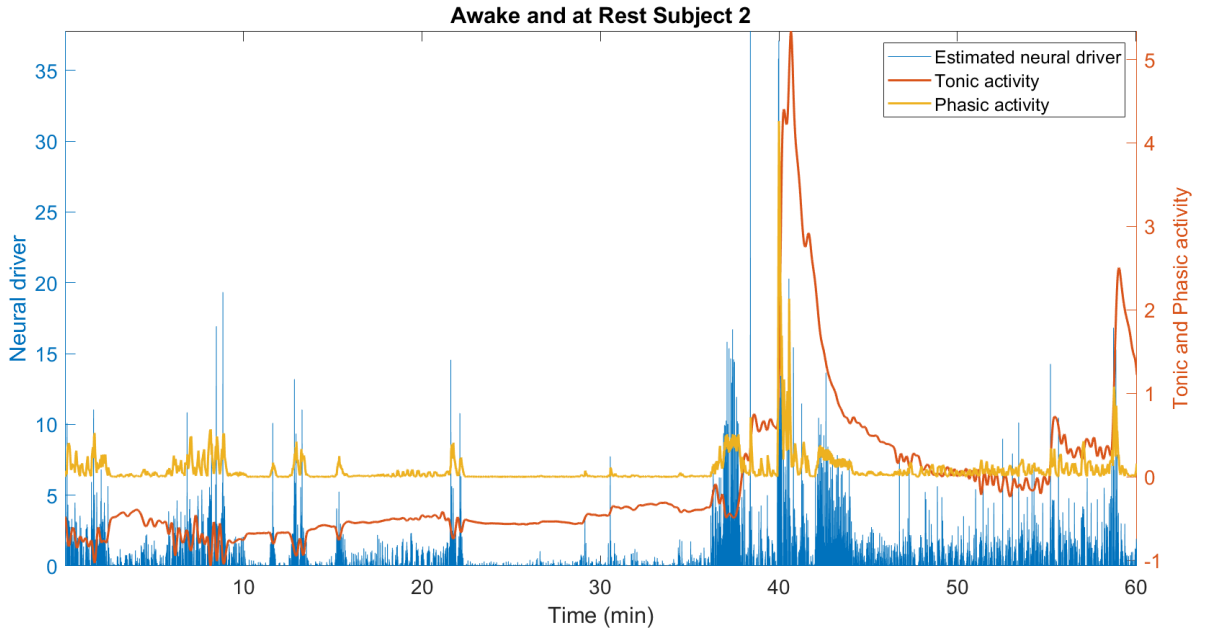


Fig. S31. Results using the cvxEDA algorithm for Subject S2 from the awake and at rest cohort, showing the tonic and phasic components and the estimated neural activity

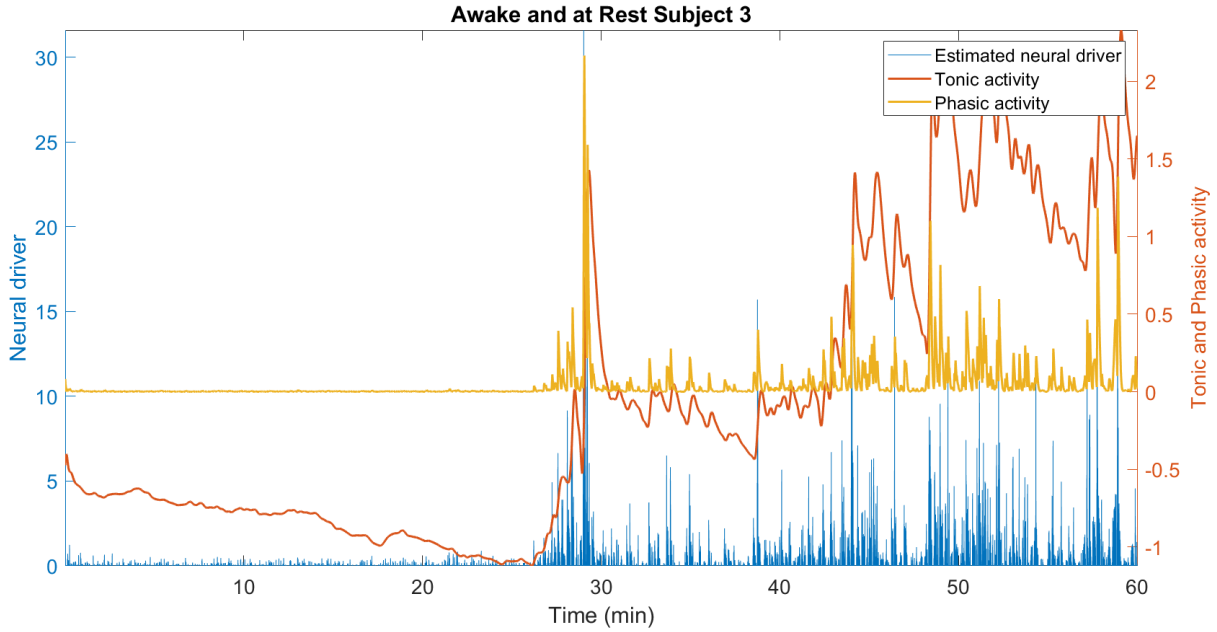


Fig. S32. Results using the cvxEDA algorithm for Subject S3 from the awake and at rest cohort, showing the tonic and phasic components and the estimated neural activity

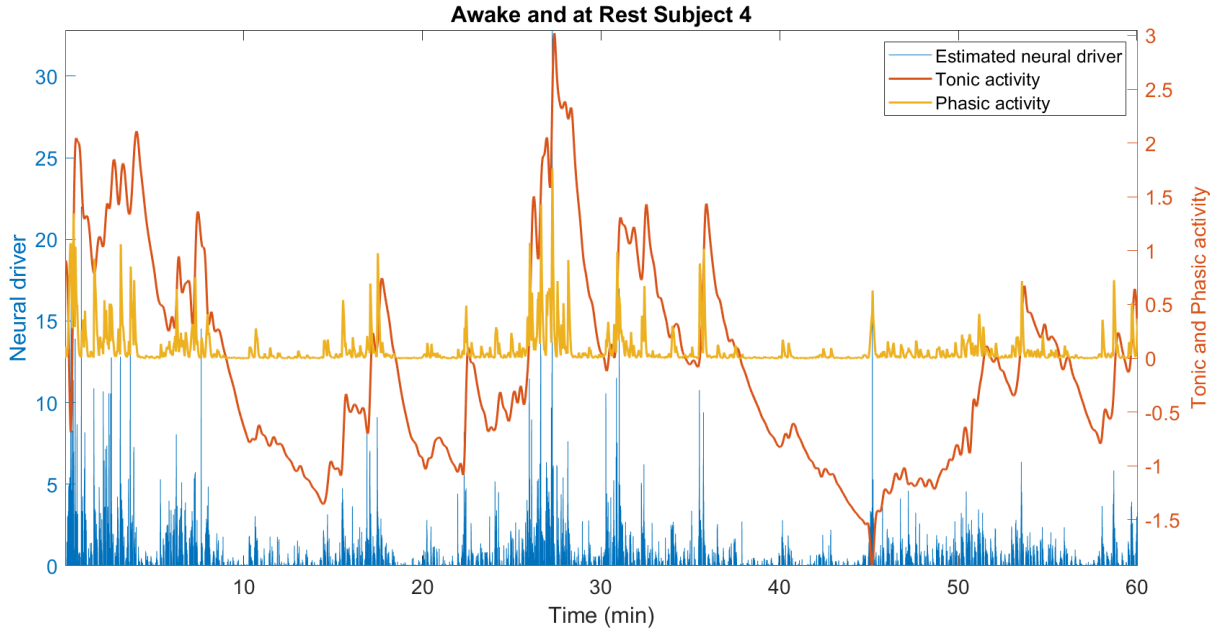


Fig. S33. Results using the cvxEDA algorithm for Subject S4 from the awake and at rest cohort, showing the tonic and phasic components and the estimated neural activity

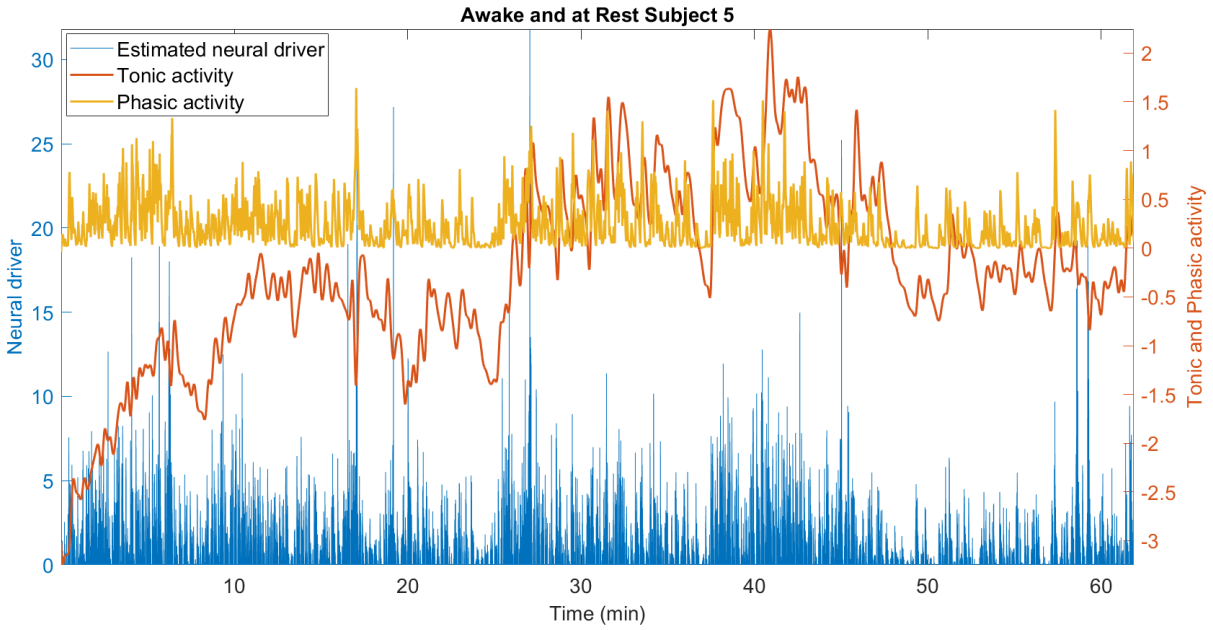


Fig. S34. Results using the cvxEDA algorithm for Subject S5 from the awake and at rest cohort, showing the tonic and phasic components and the estimated neural activity

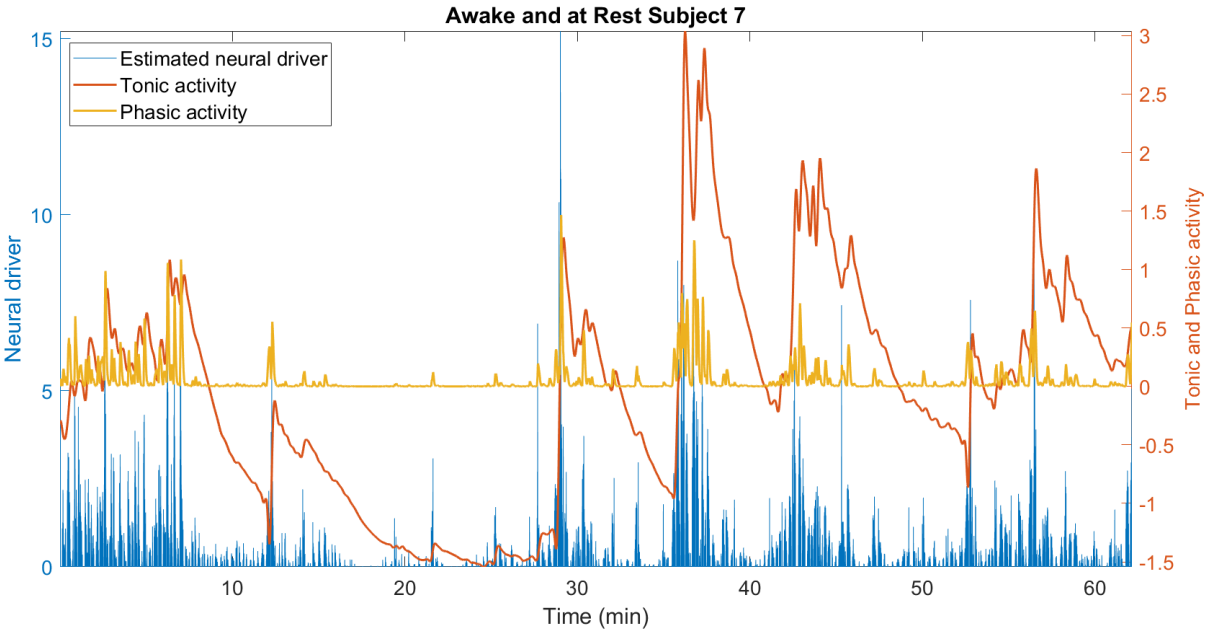


Fig. S35. Results using the cvxEDA algorithm for Subject S7 from the awake and at rest cohort, showing the tonic and phasic components and the estimated neural activity

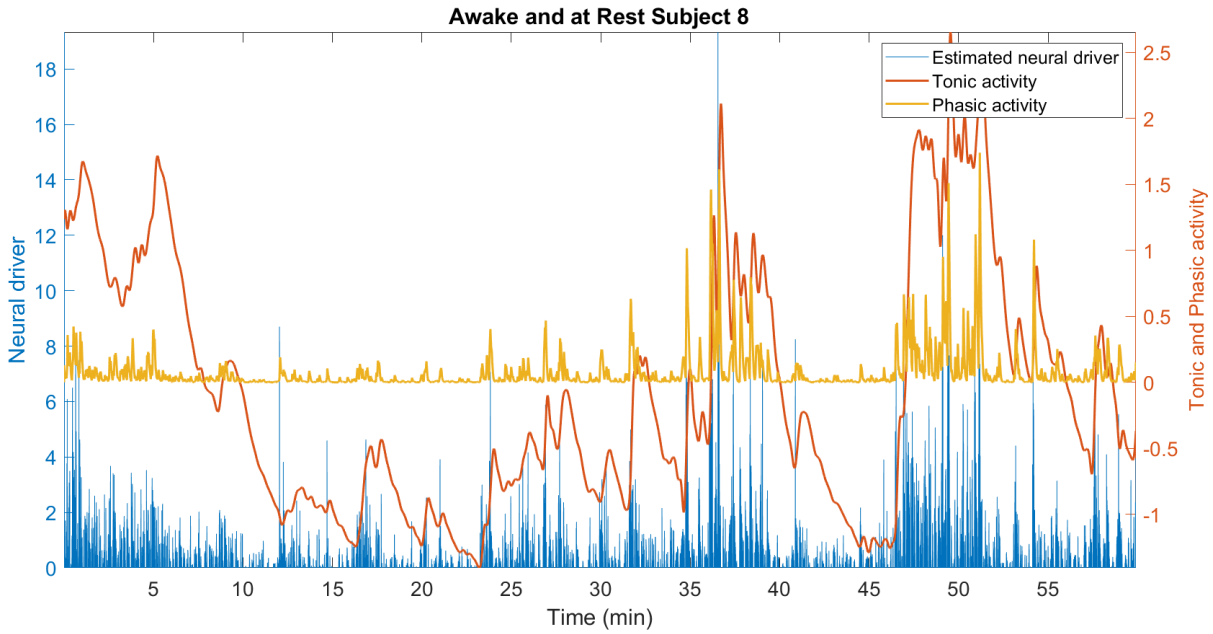


Fig. S36. Results using the cvxEDA algorithm for Subject S8 from the awake and at rest cohort, showing the tonic and phasic components and the estimated neural activity

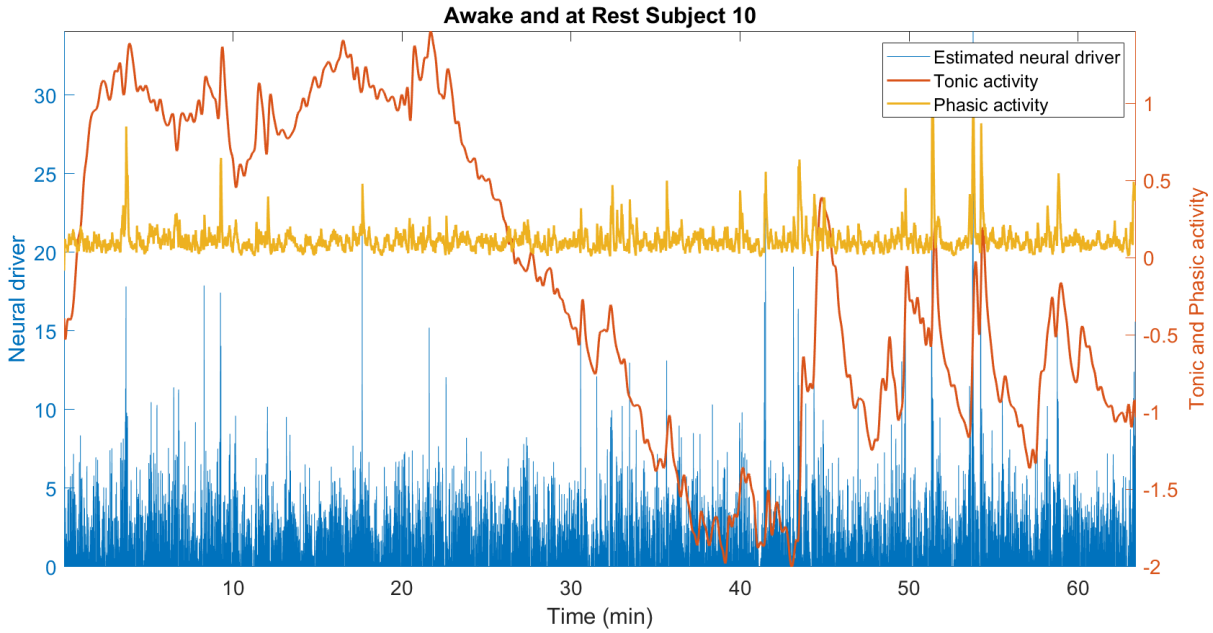


Fig. S37. Results using the cvxEDA algorithm for Subject S10 from the awake and at rest cohort, showing the tonic and phasic components and the estimated neural activity

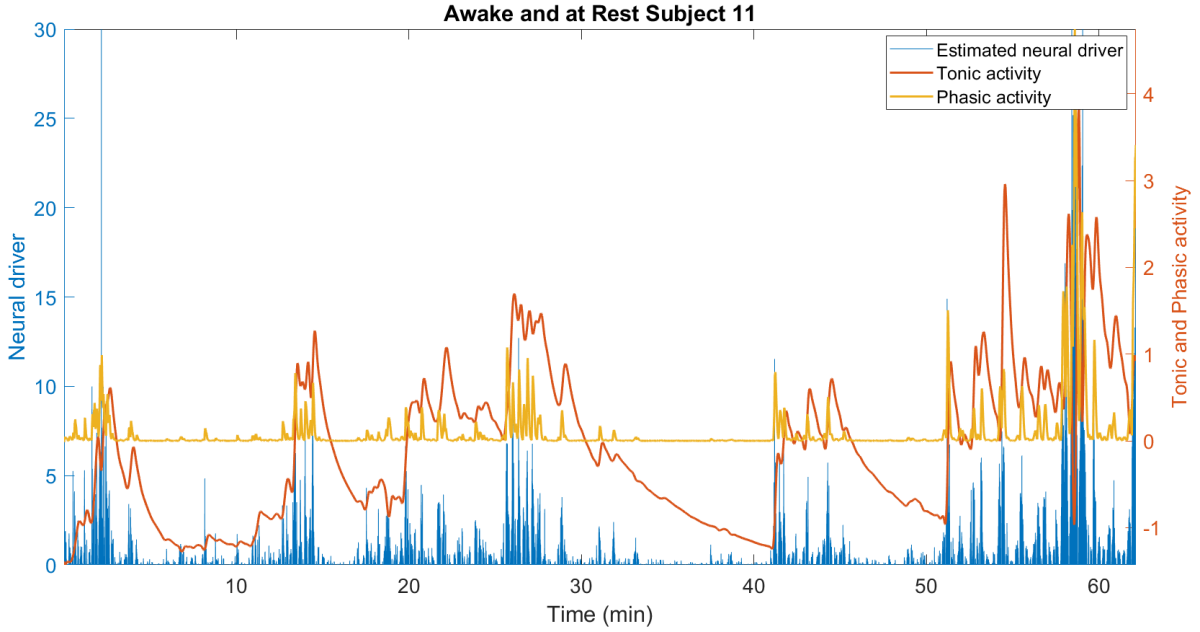


Fig. S38. Results using the cvxEDA algorithm for Subject S11 from the awake and at rest cohort, showing the tonic and phasic components and the estimated neural activity

# cvxEDA ALGORITHM RESULTS ON PROPOFOL SEDATION COHORT

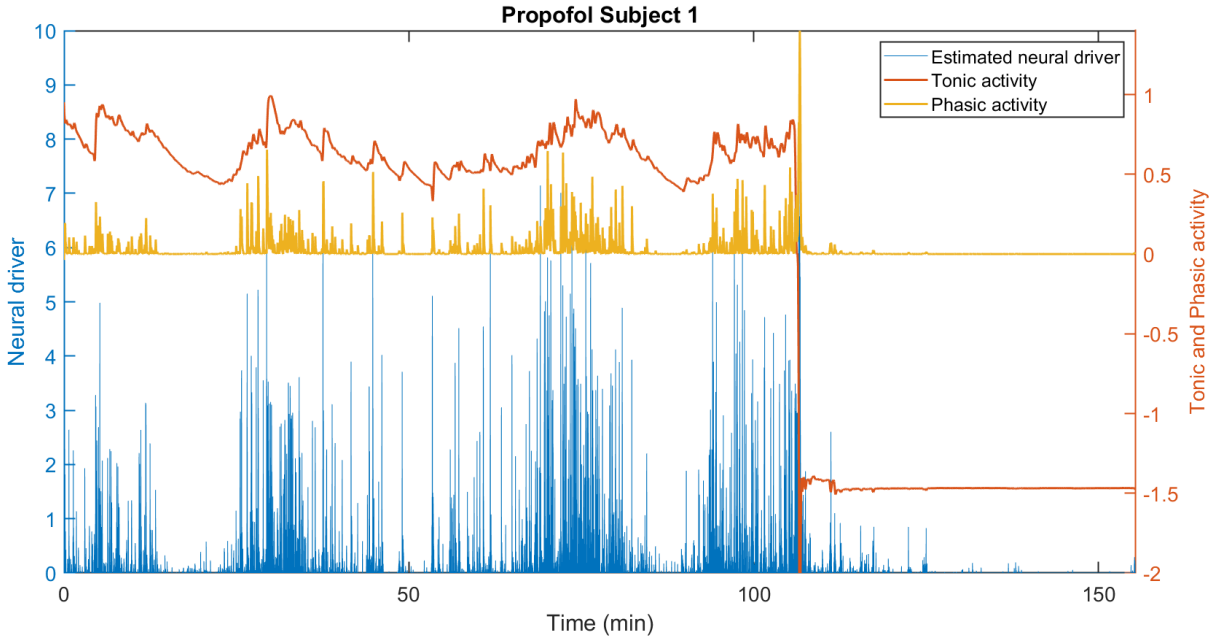


Fig. S39. Results using the cvxEDA algorithm for Subject P1 from the propofol sedation cohort, showing the tonic and phasic components and the estimated neural activity

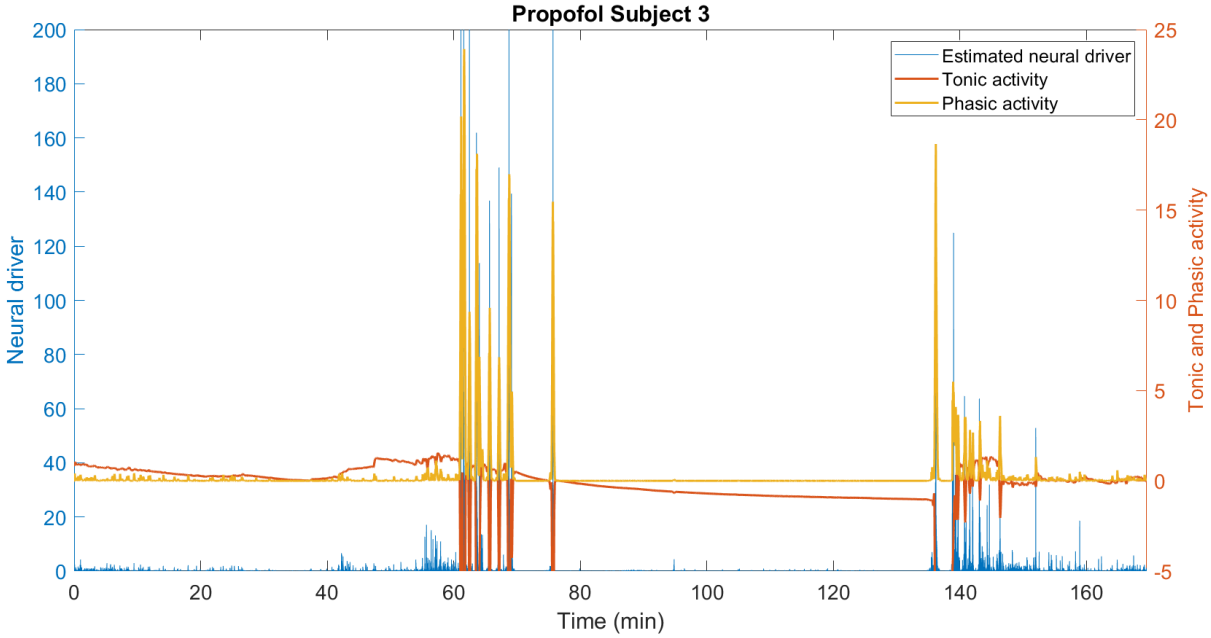


Fig. S40. Results using the cvxEDA algorithm for Subject P3 from the propofol sedation cohort, showing the tonic and phasic components and the estimated neural activity

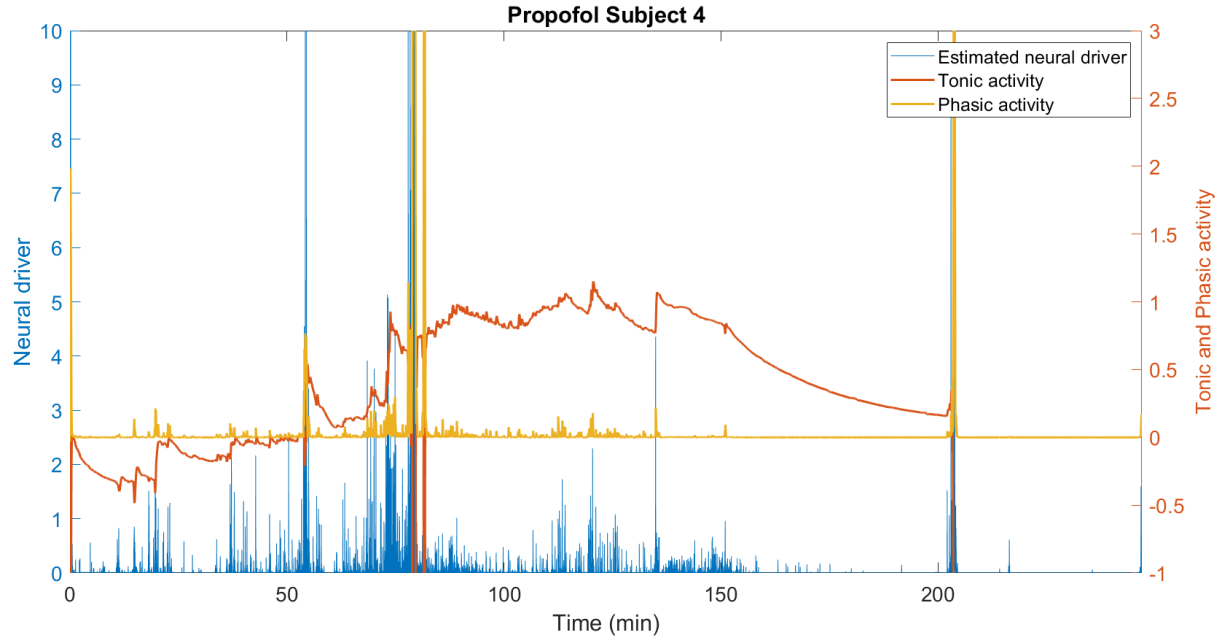


Fig. S41. Results using the cvxEDA algorithm for Subject P4 from the propofol sedation cohort, showing the tonic and phasic components and the estimated neural activity

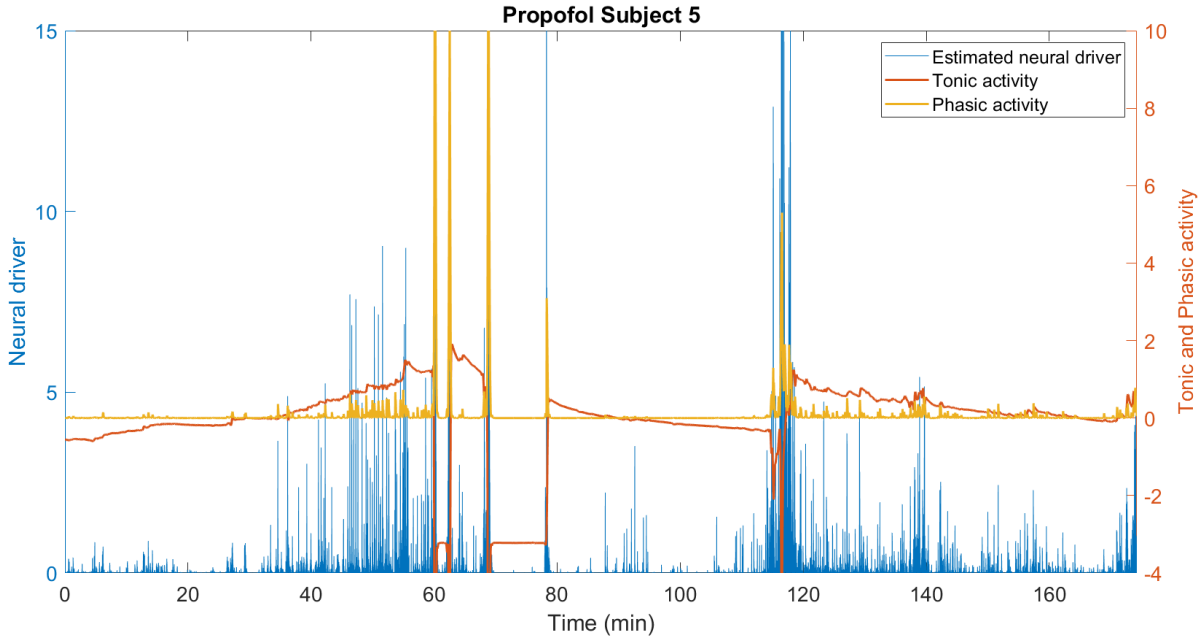


Fig. S42. Results using the cvxEDA algorithm for Subject P5 from the propofol sedation cohort, showing the tonic and phasic components and the estimated neural activity

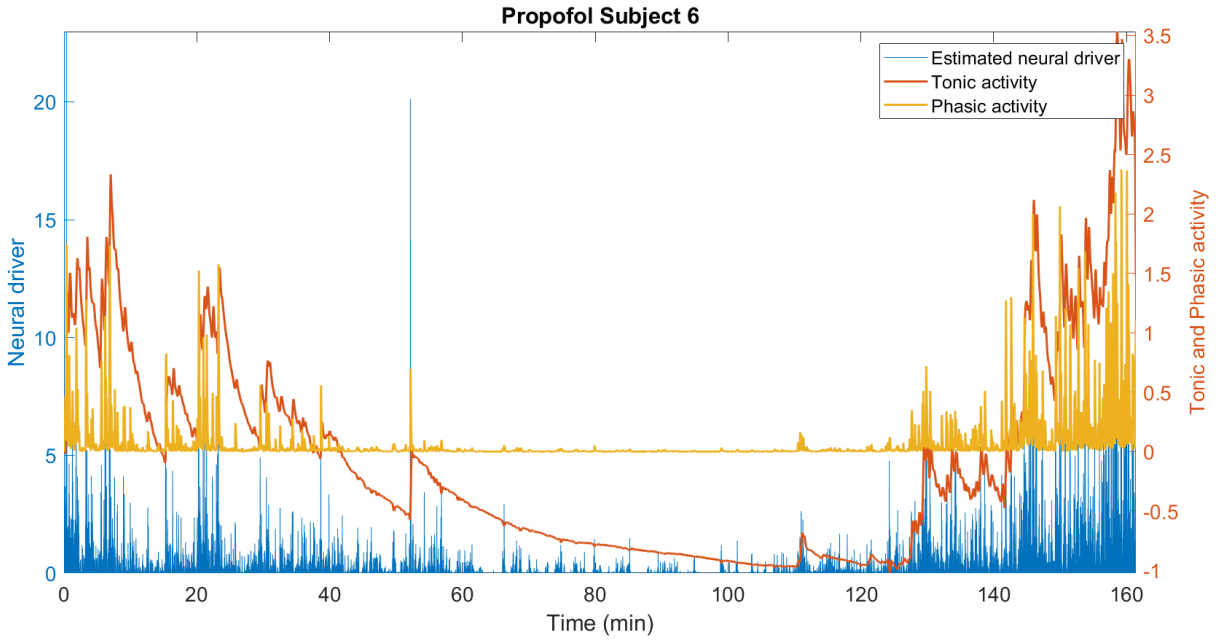


Fig. S43. Results using the cvxEDA algorithm for Subject P6 from the propofol sedation cohort, showing the tonic and phasic components and the estimated neural activity

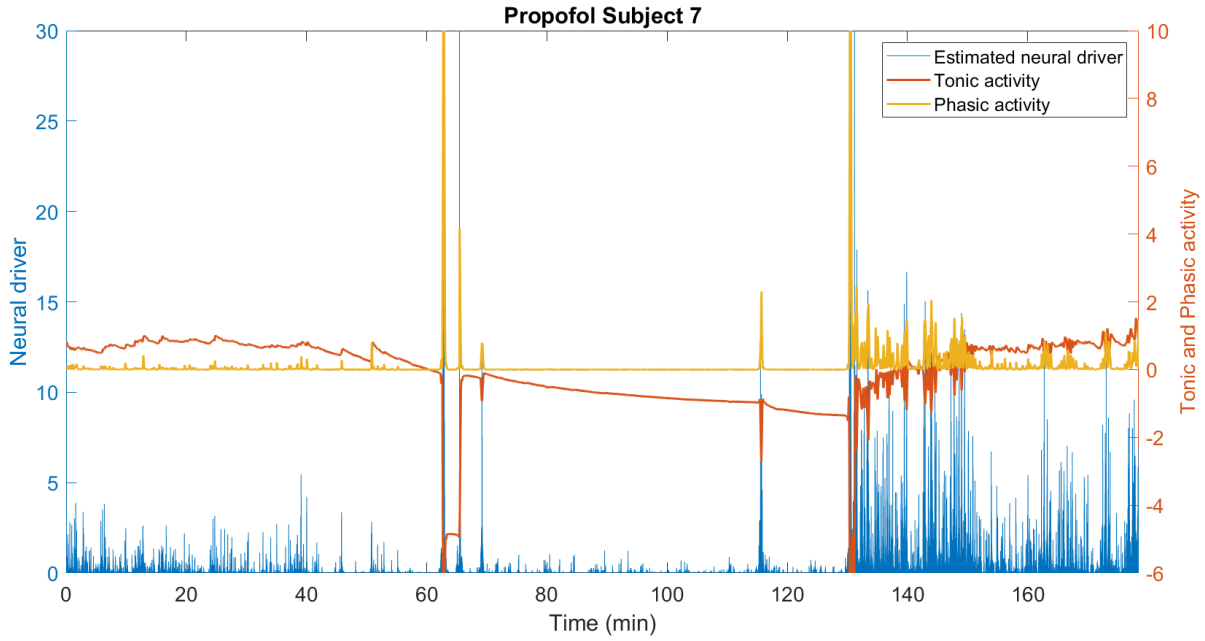


Fig. S44. Results using the cvxEDA algorithm for Subject P7 from the propofol sedation cohort, showing the tonic and phasic components and the estimated neural activity

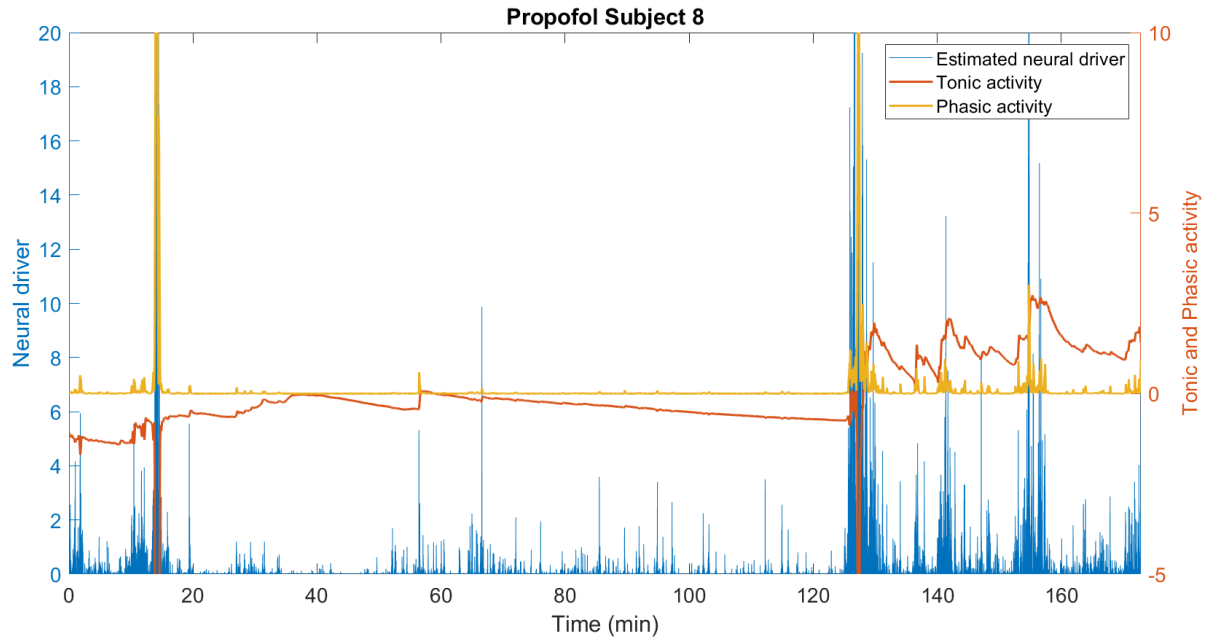


Fig. S45. Results using the cvxEDA algorithm for Subject P8 from the propofol sedation cohort, showing the tonic and phasic components and the estimated neural activity

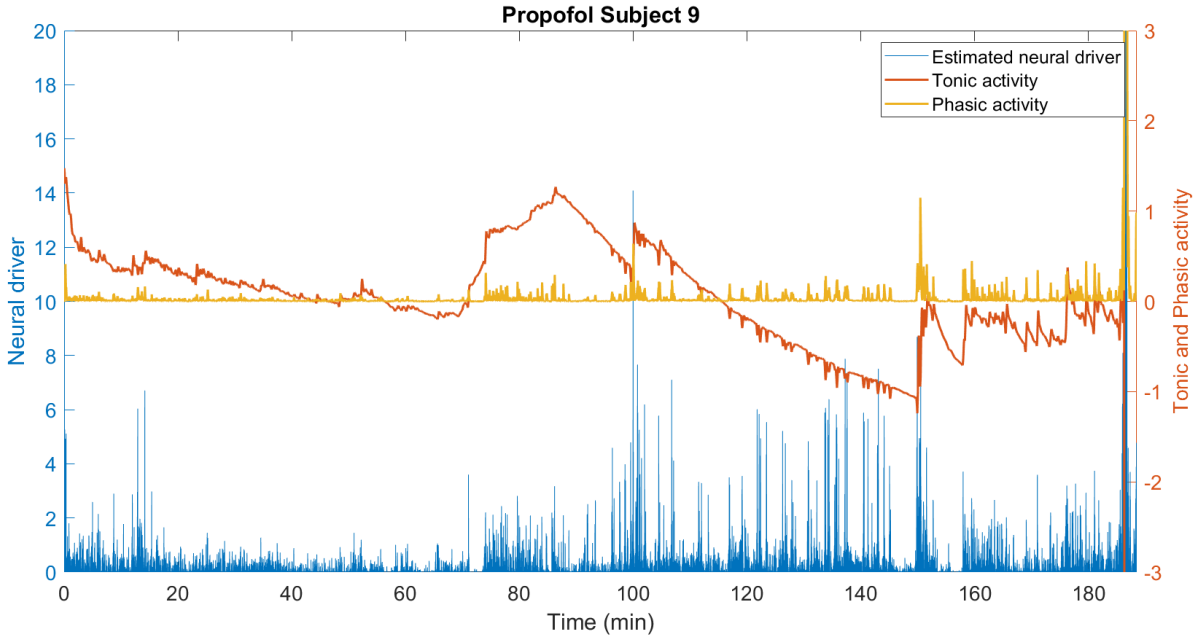


Fig. S46. Results using the cvxEDA algorithm for Subject P9 from the propofol sedation cohort, showing the tonic and phasic components and the estimated neural activity

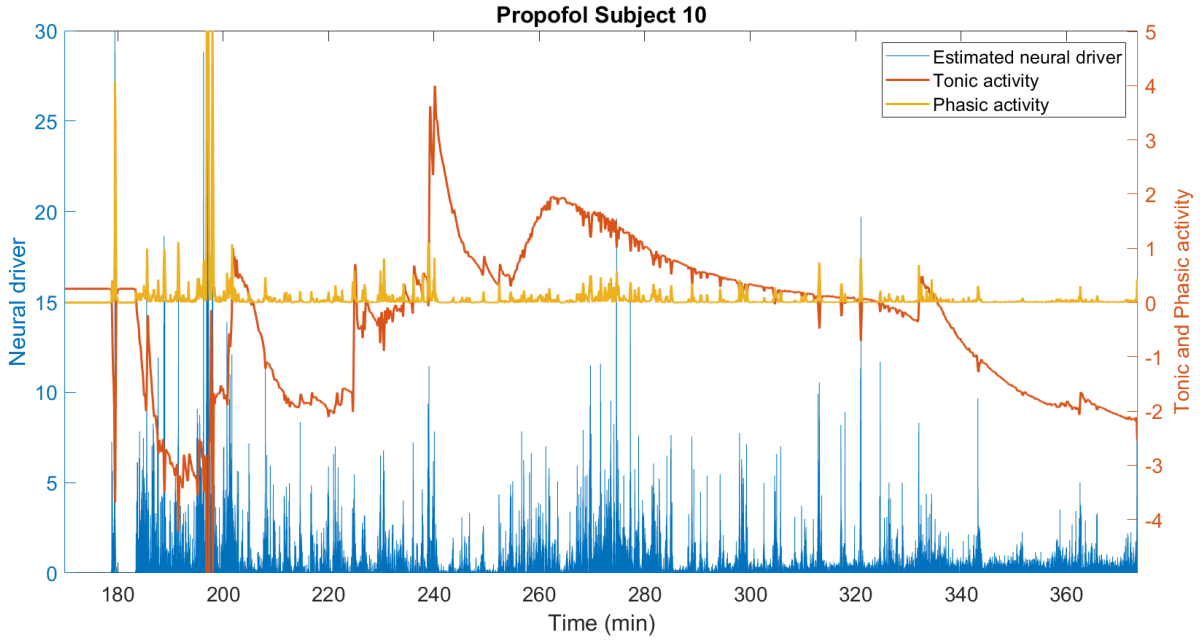


Fig. S47. Results using the cvxEDA algorithm for Subject P10 from the propofol sedation cohort, showing the tonic and phasic components and the estimated neural activity

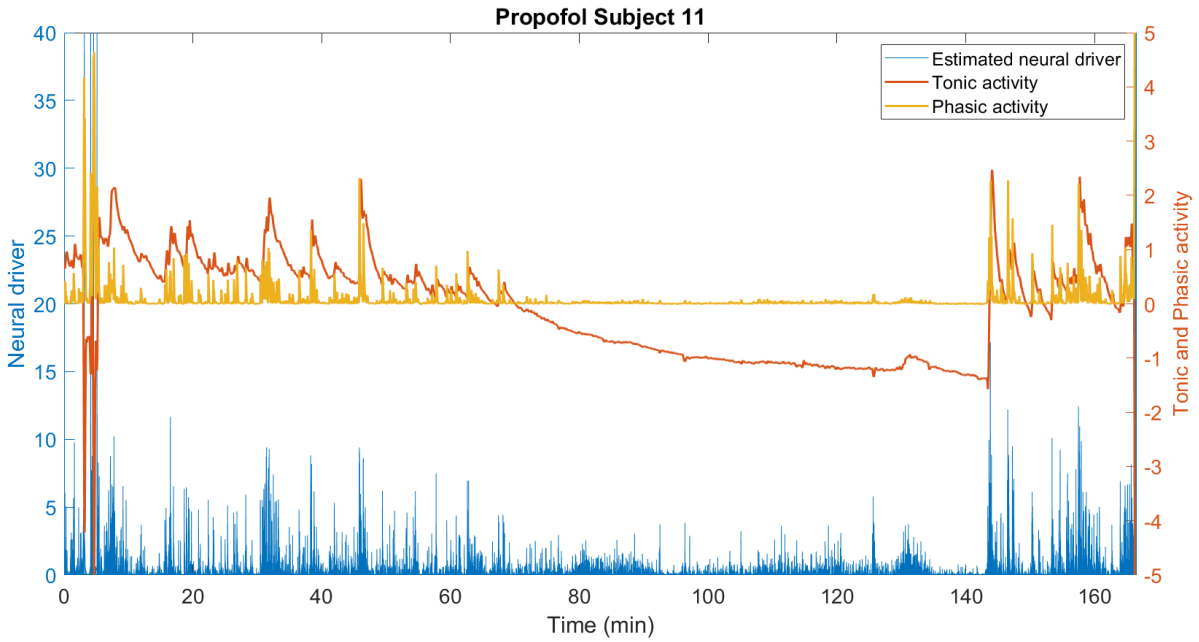


Fig. S48. Results using the cvxEDA algorithm for Subject P11 from the propofol sedation cohort, showing the tonic and phasic components and the estimated neural activity